NTNU

Norwegian University of
Science and Technology

Control of a Variable Speed Drive with a Multilevel Inverter for subsea applications

Luis Carlos Giraldo Vasquez

Master of Science in Electric Power Engineering
Submission date: June 2010
Supervisor: Lars Einar Norum, ELKRAFT
Co-supervisor: Gunnar Snilsberg, Siemens Power electronics centre

Norwegian University of Science and Technology
Department of Electric Power Engineering

Problem Description

A Variable speed drive (VSD) plays an important role not only in industrial applications but also in offshore applications, where high reliability is requested for subsea applications. Variable speed drives are commonly used for energy saving and in some applications an increasing of the productivity is achieved. The industry has begun to demand higher power equipment and for this reason the VSD technology has experienced rapid changes towards improvement. The use of multilevel inverters has emerged as the solution for working with higher voltage levels being an attractive solution to control ac drives in the megawatt range. Subsea drives have become the new trend of the drives technologies in the oil and gas sector. Currently and in order to have the drive close to the load avoiding a long cable between them, the design of new subsea technologies are relevant for the companies. Because of the importance for the oil and gas sector to have reliable systems, it is thus of interest to study the performance of two control methods for VSDs with base on speed and torque control response by the use of a simulation tool like PSIM.

Assignment given: 04. February 2010
Supervisor: Lars Einar Norum, ELKRAFT

Summary

This work deals with analyses of the control for a subsea drive with multilevel inverter. The use of those drives have become the new trend for using of pumps/compressors at minor oil and gas reservoirs located far away from existing platforms.

It is developed a general model for analyzing a variable speed drive with a multilevel inverter with the objective to verify the response of two control methods for a specific application. The simulation model is used to identify the performance of both methods in terms of speed response, torque ripple and transient behavior.

Simulation models for multilevel inverter, induction machine and both control techniques are developed. A multilevel inverter and an induction machine have been used as prototypes. The design of the controllers has shown that the whole performance of the two control schemes is comparable. Those models are developed using PSIM simulation tool.

Most of the results are related to the performance of the speed, torque ripple and transients behavior of both control methods when a 3kW 460V squirrel cage motor is fed from a cascaded H-bridge inverter.

The main difference between the two control methods can be noted in the sensitivity of the parameters and the torque ripple. The implementation of them demands accurate information on motor parameters. However, parameters such as rotor and stator resistances may vary during operating conditions due to the temperature. In that sense, modified direct torque control may have a better performance for practical implementations. However for applications where the estimation of the torque is very important, indirect field oriented control may have better results.

Preface

I would like to thank my supervisor from Norwegian University of Science and Technology (NTNU), Professor, Lars E. Norum for giving me opportunity to take a part in this project and for his help, guidance and valuable comments throughout the work. Also, I want to thank PhD student Alejandro Garces for helpful input on the models and simulations of the control methods.

My personal thanks are extended to my family and my beloved Eliana who were always there to support me and to share my thoughts in the distance. By you, I know that when there is real love, the distance is not an obstacle to keep it. My life would not be the same without you.

Finally, I would like also to thank all my friends here at NTNU for the great and unforgettable moments we had together during the last years of studies.

Again, thank you all!

Trondheim, June 2010

Luis Carlos Giraldo Vasquez

Table of Content

List of Figures

List of Tables

1. Introduction

Offshore gas and oil resources located at long distances from existing installations are often exploited by use of subsea systems. Electrically driven wellhead pumps, compressors are the current alternatives to traditional water and gas injection for pressure augmenting requirements. In this context, the use of variable speed drives plays an important role in the oil and gas industry where high reliability is requested for subsea applications. Normally variables speed drives (VSDs) are placed on the platform and it is connected to the subsea load through a long cable. Due to this long cable resonance frequencies of the system may coincide with the harmonic generated by the switching frequency of the inverter. This long cable is important to the start-up and acceleration of the induction machine. Because of the long distance (20-50km) between them real time signal feedback from the subsea load should be avoided. In order to avoid those drawbacks, the industry has begun to demand higher power equipment and for this reason a new trend for subsea drives has taken place in the oil and gas industry. Besides that VSD technology has experienced rapid changes towards improvement. The use of multilevel inverters has emerged as the solution for working with higher voltage levels being an attractive solution to control ac drives in the megawatt range. As an example, a development of a 12.5MW subsea compression station in Ormen Lange which is a gas field located 120 km off the northwest coast of Norway in water depths between 850 and 1,100 meters has been carried out.

High power inverters and medium voltage drives have been studied intensively since the mid-1980s for industrial applications [1][2]. These inverters synthesize higher output voltage levels with a better harmonic spectrum and less motor winding insulation stress. Normally the medium voltage drives are available for ratings from 0,4MW to 40MW at the medium voltage level of 2,3kV to 13,8kV as is shown in figure 1.1

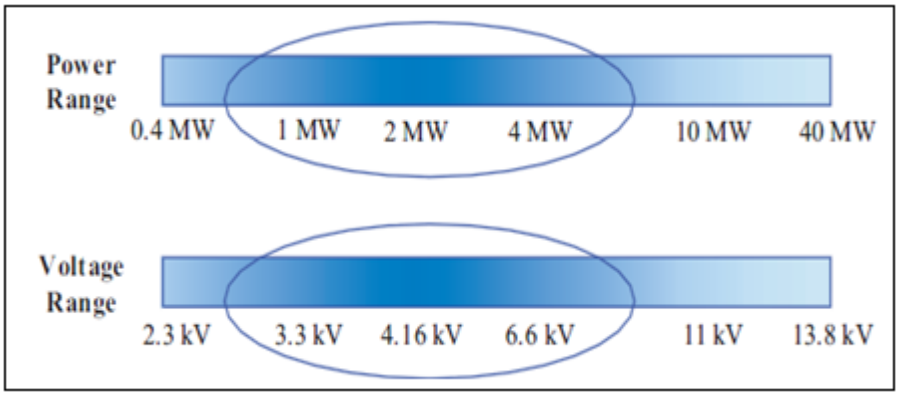

Figure 1.1 Voltage and power ranges of industrial MV drives [3]

About 85% of industrial motors are squirrel cage motor and 80% of them are connected to supply via any type of power inverters be it a soft starter or variable speed drives (VSD) [4]. In the oil and gas sector high power pumps and compressors need to medium voltage drives (MVDs). There is a large variety of inverter topologies for MVDs. Three prominent multilevel topologies are known as diode-clamped (or neutral-point-clamped) [5], flying-capacitor and cascaded multilevel inverters [6][7].

For industrial applications only 15% of the installed drives are nonstandard drives. It is reported that 97% of the currently installed medium voltage motors operate at a fixed speed and only 3% of them are controlled by variable-speed drives [4].

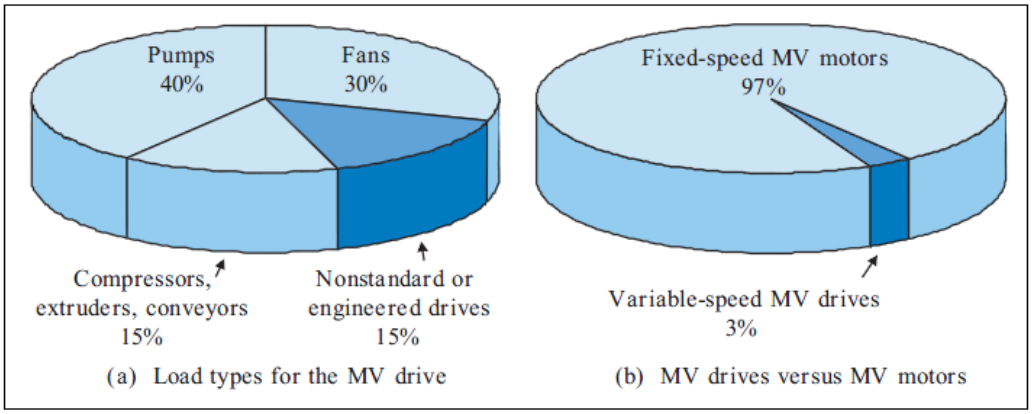

Figure 1.2 Medium voltage drives market survey [3]

1.1 Background

For drives with constant inertia, the mechanical system of the motor and its load can be described by a fundamental torque equation:

$$T = T_l + J\frac{d\omega_m}{dt} \tag{1.1}$$

where T is the instantaneous value of the developed motor torque and T_l is the instantaneous value of the load torque, ω_m is the instantaneous angular velocity of the motor shaft and J is the moment of inertia of the motor and its load. Equation (1.1) shows that the torque developed by the motor is counter-balanced by a load torque, and a dynamic torque $J\frac{d\omega_m}{dt}$ which is present only during transient operation. The drive accelerates or decelerates depending on whether T is greater or less than T_l. During deceleration, the dynamic torque has a negative sign. Therefore, it assists the motor developed torque T and maintains the drive motion by extracting energy from the stored kinetic energy. It is thus, very important to control the torque and the speed for drives for different applications. Figure 1.3, shows the typical Torque-Speed curve of the typical three-phase induction motor.

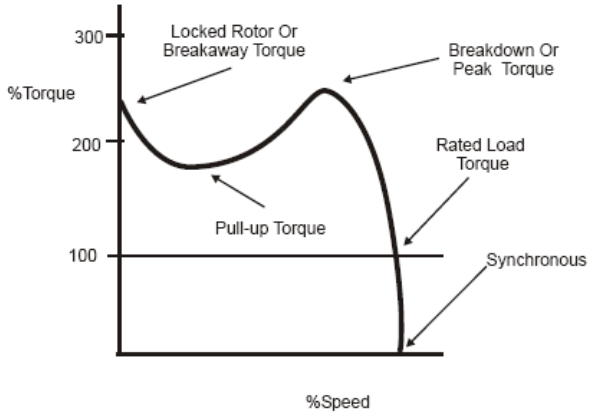

Figure 1.3 Torque-Speed curve of the typical three-phase induction motor

The control of induction machines can be divided into scalar and vector control. The general classification of the variable-frequency methods is shown in Appendix 1. In scalar control, which is based on relationships valid in steady state, only magnitude and frequency (angular speed) of voltage, current, and flux linkage space vectors are controlled. This method is somewhat easy to implement, but the coupling effect (both torque and flux are functions of voltage and frequency) gives a sluggish response. Contrarily, in vector control, which is based on relations valid for dynamic states, not only magnitude and frequency (angular speed) but also instantaneous positions of voltage, current, and flux space vectors are controlled. Thus, the vector control acts on the positions of the space vectors and provides their correct orientation both in steady state and during transients [8]. The vector control method can be implemented in several ways. The most popular methods, are the field-oriented control (FOC) and direct torque control (DTC), both methods give the induction motor high performance.

In vector control method a dynamic model of Induction Motor is made so that it takes into accounts both the transient and steady state of the machine. The main idea of the vector control of an induction machines is based on making an AC induction machine behaves as a DC machine. Basically the voltages of an AC machine represented in stator $\alpha\beta$ coordinates are transformed to synchronously rotating '*dq'* coordinates so that the PI control on AC machines can be implemented. This is because AC varying quantities in steady state will be transformed to DC quantities in the '*dq'* system. These results in a constant value in steady state on which PI control can be implemented [8].

1.2 Aim and Outline of the Thesis

The aim of this work is to give a comparison emphasizing advantages and disadvantages of the two industrial standards for induction motors control -field-oriented control and modified direct torque control- with an H-bridge cascaded multilevel inverter and an induction motor with a subsea pump as a prototype. The performance of the two control schemes is evaluated in terms of torque, speed and current ripple, and transient response to step variations of the command. The analysis has been carried out on the basis of the results obtained by numerical simulations by using PSIM software.

The thesis is arranged in seven main chapters: This introduction is followed by an overview of medium voltage inverters in chapter 2.

The scope of the work and the description of the systems used as prototypes are shown in chapter 3.

A study of H-bridge cascaded multilevel inverter on the basis of state of the art topologies, modulation techniques and some simulation results are discussed in chapter 4.

The theory of the vector control and direct torque control, as same as the features of the main schemes to control induction machines developed in the work are presented in chapter 5.

The main simulation results and a comparison of the different control schemes based on their performance are shown in chapter 6. The conclusion and discussion are presented in chapter 7. Finally a future work is proposed in chapter 8.

1.3 References

[1]. T. A. Meynard and H. Foch, "Multi-level Conversion: High Voltage Choppers and Voltage-source Inverters" Proceedings of the IEEE Power Electronics Specialist Conference, 1992, pp. 397-403.

[2]. J. S. Lai and F. Z. Peng, "Multilevel converters - A new breed of power converters" IEEE Transaction Industry Applications Conference, May-June 1996, vol. 32, pp. 509-517.

[3]. Bin Wu, "High-Power Converters and ac Drives" ISBN**:** 9780471731719 , DOI: 10.1002/0471773719 Copyright 2006, the Institute of Electrical and Electronics Engineers, Inc.

[4]. S. Malik and D. Kluge, "ACS 1000-World's first standard AC drive for medium-voltage Applications" ABB Rev., 1998, no. 2, pp. 4-11.

[5]. A. Nabae, I. Takahashi, and H. Akagi, "A new neutral-point clamped PWM inverter" IEEE Transactions on Industrial Applications, vol. IA-17, pp. 518–523, Sept./Oct. 1981.

[6]. J. S. Lai and F. Z. Peng, "Multilevel converters–A new breed of power converters," IEEE Transactions on Industrial Applications, vol. 32, pp. 509–517, May-June 1996.

[7]. G. Beinhold, R. Jacob, and M. Nahrstaedt, "A new range of medium voltage multilevel inverter drives with floating capacitor technology," Proc. European Power Electronics Conf, 2001.

[8] G. S. Buja, M. P. Kazmierkowski "Direct torque control of PWM inverters AC motors-A survey", IEEE Transcations on Industrial Electronics, vol. 51, no. 4, pp. 744-757. August 2004.

2. Medium Voltage Drives Background

This chapter provides a brief background concerning the effects of the long cables for offshore motor drive applications and an overview of medium voltage inverters based on it is state of art is also presented.

2.1 Effects of Long Cables for Offshore Applications

Because of the increasing of the reservoirs of oil and gas that have been found in the ocean, pumping oil from these reservoirs is a challenge that the oil industry is facing today. Subsea cables have been used to feed subsea systems from sources on the topside. However, due to wide applications of variable speed drives (VSDs) in offshore applications, the system normally contains a certain amount of harmonic currents. These harmonics could interact with subsea cables and cause parallel resonance and large harmonic distortions in offshore systems [1]. Normally subsea pumps are efficient in producing oil of gas [2]. And according with [3] practically the unique issue for ESP systems is inaccessibility after installation. Therefore, it is very important to guarantee high reliability in the ESP system performance.

2.2 Application Issues for Drives

A typical configuration of a variable speed drive driving a subsea pump using long cable leads is shown in figure 2.1.

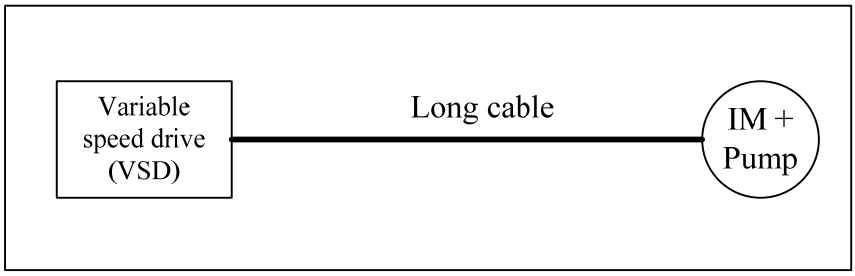

Figure 2.1 Variable speed drive driving a subsea pump using long cable leads

- Long cable lengths contribute to a damped high-frequency ringing at the motor terminals due to the distributed nature of the cable leakage inductance and coupling capacitance (L-C), which result in overvoltage and further stress the motor insulation.

- Variable speed drives provide flexible control on the operation of subsea systems with typical operating frequency ranging between 50 and 70 Hz, but the harmonics generated at the output of a VFD could interact with the subsea cable and create a series resonance condition at the load side of the drive [4].

- The impedance of the subsea cable could introduce a significant voltage drop during motor starting and cause the motor starting difficulty if the subsea pump system is not properly designed.

- On long cables PWM pulses traveling between the inverter and the motor behave like traveling waves on transmission lines. Forward-traveling waves, or PWM pulses, travel from the inverter to the motor, while backward- traveling waves move toward the inverter due to voltage reflection.

- Voltage reflection is a function of inverter output pulse rise time and the length of the motor cables, which behave as a transmission line for the inverter output pulses. The PWM pulses travel at approximately half the speed of light (150-200m/μs), and if the pulses take longer than half the rise time to travel from the inverter to the motor, then a full reflection will occur at the motor and the pulse amplitude will approximately double [5].

- Filters are needed in order to reduce the adverse effects of the long cable. Some filters are designed to terminate the long lead cable with the cable surge impedance to reduce over voltage reflections, ringing and the *dv/dt* at the motor terminals [6].

- Because of the issues and drawbacks of using long cables between the variable speed drive and the subsea system described above, some companies have started working on subsea medium voltage variable speed drives. Because of after installation is hard to access to the system, it is necessary to guarantee a high reliability for these kind of drives.

2.3 Overview of Medium Voltage Drives

Recently Voltage source multilevel inverter topologies have drawn tremendous interest in the power industry because of they can be extended the application of power electronics systems to higher voltage and high power ratios. The application of multilevel inverters has been very attractive for medium to high voltage range (2-13kV) applications such as: motor drive systems [7], power distribution, power quality and power conditioning applications [8]. The advantages of the multilevel inverters compared to conventional two-level inverters can be summarized as: higher voltage capability, reduction of input and output harmonic content, lower switching losses, higher amplitude fundamental and lower *dv/dt*. However, some disadvantages of multilevel inverters include voltage unbalance difficulties, unequal current stresses, and higher implementation cost and a reduction of the reliability and efficiency of the inverter the due to an increasing number of devices.

Today there is a wide variety of inverters for medium voltage drives. For low and medium power industrial applications the majority of the drive manufacturers offer different topologies of voltage source inverters, those topologies are discussed in the next section.

2.3.1 Medium Voltage industrial drives

Three main topologies of multilevel inverters have been successfully implemented as standard products for medium voltage industrial drives: the Three-Level Neutral Point Clamped [9], the Four-Level Flying Capacitor [10], and the cascaded H-Bridge [11]. In medium voltage applications, the Three-Level Neutral Point Clamped topology has been accepted by several manufacturers such as ABB which is using this topology in both their ACS 1000 [12] and ACS 6000 series. The Four-Level Flying Capacitor is attractive if a very high switching frequency, a low harmonic distortion, and a small output filter or a high output voltage is required [13]. One of the manufacturers of drives Alstom, has adapted this topology for VDM 6000 series.

The cascaded H-bridge topology uses low-voltage blocking devices (e.g. 1700V IGBTs) with a high switching frequency capability. It typically consists of three to six equal H-bridge cells per phase, which results in a seven to thirteen levels output voltage waveform. Perfect harmony developed by Siemens uses this kind of topology [14].

Figure 2.2 shows the pictures of an medium voltage drive (4,6kV, 1,2 MW) composed by a three level neutral point clamped developed by ABB (left) and a cascaded H-bridge topology developed by Siemens (right).

Figure 2.2 Left: Three level neutral clamped inverter (ACS1000) and right: Cascaded H-bridge inverter (Perfect harmony)

Table 2-1 summarizes the available industrial medium voltage drive applications offered by drive manufactures [15]. Normally the medium voltage drives cover power ratings from 0.2MW to 40MW at the medium voltage level of 2.3kV to 13.8kV.

Manufacterer	Type	Power (MVA)	Topology
ABB	ACS 1000	0,3-5	Three level neutral point clamped
	ACS 5000	5,2-24	Multilevel cascaded H-bridge inverter
	ACS 6000	3,0-27	Three level neutral point clamped
Allen Bradley	Power Flex 7000	0,15-6,7	Current source inverter (CSI)
Alstom	VDM 5000	1,4-7,2	Two level voltage source inverter
	VDM 6000	0,3-8	Four level flying capacitor
	VDM 7000	7-9,5	Three level neutral point clamped
General Electric	Dura-Bilt5 MV	0,3-2,4	Three level neutral point clamped
	MV-GP Type H	0,45-7,5	Multilevel cascaded H-bridge inverter
Siemens	Perfect Harmony	0,2 - 31	Multilevel cascaded H-bridge inverter
	Simovert-MV	0,6 - 7,2	Three level neutral point clamped
	Simovert-S	≥10	Load commutated inverter

Table 2.1 some of the available industrial medium voltage drives on the market [15]

2.4 References

[1]. K. S. Smith and L. Ran, "Active filter used as a controlled reactance to prevent harmonic resonance in interconnected offshore power systems" Proc. Inst. Elect. Eng. Gener. Transm. Distrib., vol. 146, no. 4, pp. 393– 399, Jul. 1999.

[2]. R. Yacamini, W. Phang, P. Brogan, A. Scott, "Variable speed drives for remote downhole pump applications," Power Eng. J, vol. 14, no. 1, pp. 29–36, Feb. 2000.

[3]. A. C. S. de Lima, R. M. Stephan, A. Pedroso, and J. Mourente, "Analysis of a long distance drive for an induction motor," in Proc. IEEE ISIE, Jun. 17–20, 1996, vol. 2, pp. 867–872.

[4]. X. Liang, S.O Faried, O. Ilochonwu "Subsea cable applications in electrical submergible pump systems" IEEE Transactions on industry applications. Vol 46. no 2, pp 575-583 March-April 2010.

[5]. A. von Jouanne, P. Enjeti W. Gray "The effect of long motor leads on PWM inverter fed AC motor drive systems" IEEE APEC Conf , 1995.

[6]. A. von Jouanne, D. Rendusara, P. Enjeti, W. Gray, "Filtering techniques to minimize the effect of long motor leads on PWM inverter fed AC motor drive systems," in Conf. Rec. 30th IEEE IAS Annu. Meeting, Oct. 8–12, 1995, vol. 1, pp. 37–44.

[7]. P.K. Steiner and M.D. Manjrekar, "Practical Medium Voltage Converter Topologies for High Power Applications," IEEE IAS Conference records, Vol. 3, pp. 1723-1730, 2001.

[8]. C.K. Lee, J.S.K. Leung, R. Hui and H.S. Chung, "Circuit-Level Comparison of STATCOM Technologies," IEEE Transactions on Power Electronics, Vol. 18, No.4, pp. 1084-1092, July 2003.

[9]. M. Buschmann and J. Steinke, "Robust and reliable medium voltage PWM inverter with motor friendly output," in Proc. European Power Electronics Appl. Conf., 1997, vol. 3, pp. 502-507.

[10]. G. Beinhold, R. Jacob, and M. Nahrstaedt, "A new range of medium voltage multilevel inverter drives with floating capacitor technology," Proc. European Power Electronics Conf., 2001.

[11]. P. W. Hammond, "A New Approach to Enhance Power Quality for Medium Voltage ACDrives," IEEE Trans. on Ind. Appl., January-February 1997, vol. 33, no. 1.

[12]. S. Malik and D. Kluge, "ACS 1000—World's first standard AC drive for medium-voltage Applications," ABB Rev., 1998, no. 2, pp. 4-11.

[13]. S.S. Fazel, D. Krug, T. Taleb, and S. Bernet, "Comparison of Power Semiconductor Utilization, Losses and Harmonic Spectrum of State-of-the-Art 4.16kV Multi-Level Voltage Source Converters," in EPE Conf. Rec., Dresden, Germany, 2005.

[14]. Siemens drives website: www.automation.siemens.com

[15]. S. Bernet, "State of the Art and Developments of Medium Voltage Converters – An Overview," Przeglad Elektrotechniczny (Electrical Review), May 2006, vol. 82, no. 5, pp. 1-10.

3. Scope of the Work

This chapter describes some considerations made during the realization of the project and the main description of the systems used to carry out the present thesis.

3.1 Initial Considerations

At the beginning of the project it was proposed to work on control of subsea drives using predictive control. The idea consisted in compare two control techniques: a conventional field oriented control and a field oriented based on predictive control. During the last decade lots of publications on predictive control have been published. Some of them are improvements or enhancements of control methods published earlier [1], whereas other authors have proposed new ideas [2][3], but even these in most cases are further developments or combinations of fundamental predictive control algorithms. The typical configuration of a predictive controller is shown in figure 3.1.

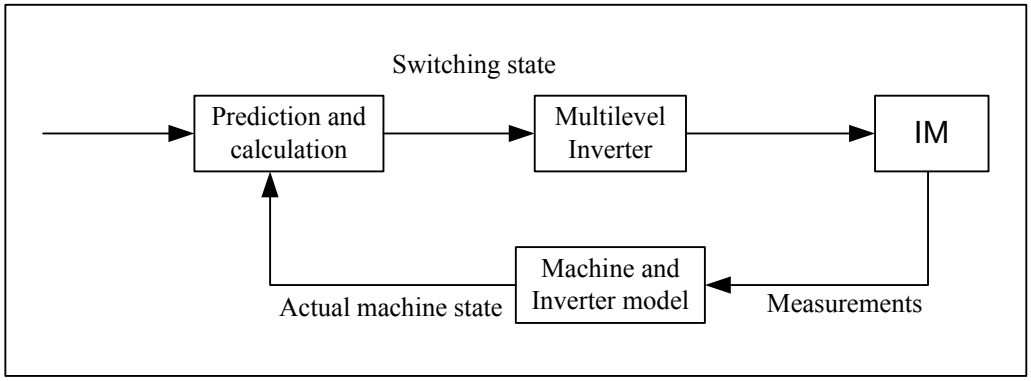

Figure 3.1 Typical configuration of a predictive controller

The figure shows that the state variables (chosen measurements) of the drive are fed into a model of the machine and the multilevel inverter. The information derived from the model is given to a block called “prediction and calculation”. This block can be regarded as the heart of a predictive control system. Comparing the actual machine state with the reference value of the drive position, the correct switching state of the inverter will be chosen corresponding to the implemented optimizing criteria, for example can be the minimum switching frequency, the minimum current distortion or the minimum torque ripple [4] [5] [6].

From a literature review it was found that, there are several predictive control strategies and they can be divided in three main groups hysteresis based, trajectory based and model based predictive control. The different family of strategies belonged to these main groups are shown in figure 3.2.

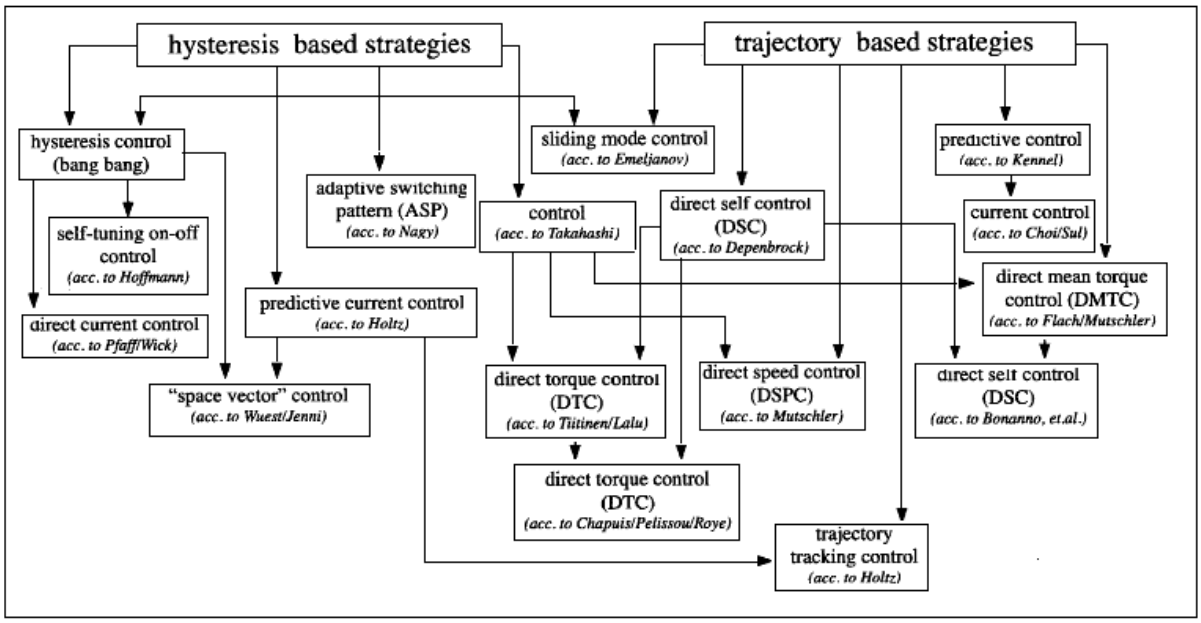

Figure 3.2 Family strategies based on predictive control [4]

Control methods with trajectory or hysteresis based algorithms are intensively related to each other. Model based control is founded on completely different strategies and forms a family of its own. With base on the above description of predictive control and the literature review made at the beginning of the present work, two reasons allowed giving up the idea of working with predictive control. Firstly the implementation of this method is complex when multilevel inverters are used, because of the number of switching states generated [7]. The other reason was the weak mathematical background related to solve optimization problems [8][9]. The most relevant literature found related to this topic was based on PhD dissertation thesis and papers [10][11][12]. Therefore, the main conclusion in the first period of the thesis was that the time to develop these ideas in the project (six months) was not long enough and thus, other methods were explored to control drives and they are described in the following chapters.

3.2 System Description

As the aim of the work is to compare two control methods for a drive with a multilevel inverter with a subsea pump as a load (see figure 3.3), the description of the elements used in the project is presented below.

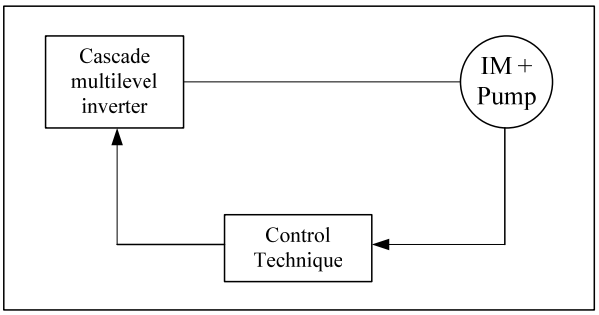

Figure 3.3 Description of the system

3.2.1 Induction Motor

The subsea load is composed by a three phase induction motor and a pump configuration, it normally is called ESP (Electric submergible pump). Due to the narrow confines in which this motor must be used, the motor construction is very specialized. It is also common to connect multiple smaller motor / pump configurations in series to achieve the necessary power and torque required to meet the necessary flow rates. The conditions in which these motors and pumps must operate are also extreme. High temperatures and pressures are to be expected as well as the corrosive nature of the materials pumped which can not only contain a high sand content but other materials as well required in the process such as CO2 [13]. A three phase induction motor is used as a prototype in the present theoretical work. Parameters are shown in table 3.1.

Parameter	Value
Rated output power (kW)	3
Frequency (Hz)	50
Rated voltage (V)	460
Rated speed (RPM)	1460
Stator winding resistance (Ω)	0,294
Stator winding leakage inductance(mH)	1,39
Rotor winding resistance (Ω)	0,156
Rotor winding leakage inductance (mH)	0,74
Magnetizing inductance (mH)	41
No of Poles	4
Rated torque	36Nm
Moment of Inertia (kg m²)	0,05

Table 3.1. Parameters of the induction motor

3.2.2 Load Torque

The load on the motor shaft is a subsea pump which is variable torque load and the required torque to drive the load increases proportional to the square of speed. Disregarding the torque behavior for starting periods, the relationship between speed and torque is illustrated in Figure 3.4.

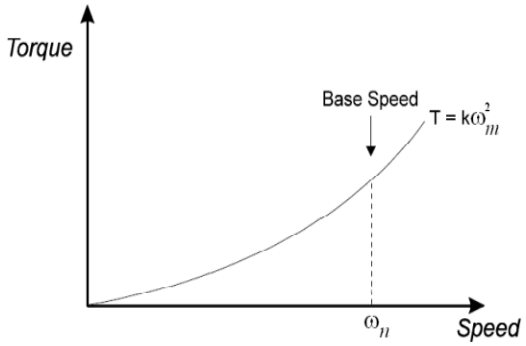

Figure 3.4 Typical Torque-Speed characteristics of a pump

The constant *K* can be found by the relation of the rated torque and the nominal speed. Due to an increase in the fractional oil volumes the load torque can vary. Therefore some variations in the torque are taken into account in order to evaluate the performance of the controller. Numerical values and more details about the load are studied in more detail in chapter 6.

3.2.3 Multilevel Inverter

With base on the description of the main industrial drives made in chapter 2, and for modulation simplicity a five level cascaded H-bridge is chosen as the inverter topology of the drive. Although this topology is not commercial, the theoretical analysis made in the work can be extended for other topologies. A single phase of this topology is shown in figure 3.5

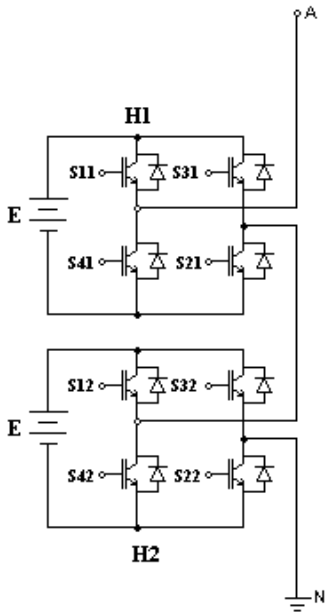

Figure 3.5 Single phase five- level cascade H-bridge inverter

With *E*=190V generating five level voltages per phase, carrier frequency of 10kHZ and assuming ideal IGBTs, it is possible to supply the motor described in section 3.2.1. A better understanding of modulation techniques and features of this topology theory is described in chapter 4.

3.2.4 Control Techniques

For drives located on the topside and connected to the load through a long cable, a rotor position indicator is used. With the measurements of the amplitude of the stator and rotor current and the rotor position, vector control can be used. Using vector control the speed and torque can be controlled independently and the current and voltage harmonics can be kept at a low level. Normally the motor currents and voltages and the rotor position are measured by using an advanced estimation state of the cable and induction motor parameters. The vector control can be extended for subsea drives and is the aim of this thesis to compare to different control techniques performance. Nowadays direct torque control and field oriented control have been widely used in industry applications. Those methods are studied in detail in chapter 5 and main simulation results are presented in chapter 6.

3.3 References

[1]. Purcell, P. Acarnley, “Multilevel hysteresis comparator forms for direct torque control schemes”, Electronic Letters, vol. 34, no. 6, pp. 601-603, March 1998.

[2]. E. Flach, R. Hoffmann, P. Mutschler, “Direct Mean Torque Control of an induction motor”, in Conf Record EPE’97, vol. 3, pp. 672-677, Trondheim 1997.

[3]. A. M. Trzynadlowski, M. M. Bech, F. Blaabjerg, J. K. Pedersen, “An integral space-vector PWM technique for DSP-controlled voltage- source-inverters”, IEEE Transactions on Industry Applications.

[4]. R. Kennel, A. Linder, “Predictive Control of Inverter Supplied Electrical Drives”, 31st IEEE Power Electronics Specialists Conference pesc'00. Vol. 2, pp. 761-766. Gahiay. 2000.

[5]. T. Geyer, G. Papafotiou, and M. Morari, “Model Predictive Direct Torque Control – Part I: Algorithm, Concept & Analysis,” IEEE Trans. on Industrial Electronics, vol 56.No 6, June 2009.

[6]. T. Geyer, “Model Predictive Direct Torque Control minimizing Switching Losses,” submitted to the 48th IEEE Conf. on Decision and Control, 2009.

[7]. Y. Wang, H. Li, X. Shi “Direct Torque Control with Space Vector Modulation for Induction Motors Fed by Cascaded Multilevel Inverters” Key Laboratory of Power System Protection and Dynamic, North China Electric Power University.

[8]. A. Bemporad, M. Morari, V. Dua, E. N. Pistikopoulos, “The explicit solution of Model Predictive Control via multiparametric quadratic programming”, American Control Conference ACC2000, pp. 872–876, Chicago, 2000.

[9]. L. Cooper, D. Steinberg, “Introduction to methods of optimization”, Philadelphia, PA: W. B. Saunders, 1970.

[10]. T.Geyer “Low Complexity Model Predictive Control in Power Electronics and Power Systems” PhD dissertation thesis, ETH No, 15953, 2005.

[11]. J. Rodrıguez, J. Pontt, C. Silva, P. Cortes, S. Rees, and U. Ammann, “Predictive direct torque control of an induction machine,” EPE-PEMC 2004 (Power Electronics and Motion Control Conference), Riga, Latvia, 2-4 September 2004.

[12]. M. A. Perez, P. Cortes, and J. Rodriguez, “Predictive control algorithm technique for multilevel asymmetric cascaded h-bridge inverters,” IEEE Transactions on Industrial Electronics, vol. 55, no. 12, pp. 4354–4361, Dec. 2008.

[13]. H. Kirby, R. Paes, J. Flores “Speed control of electric submersible pumps, the current approach”, paper No IAS54p1. IAS 2005.

4.Cascaded H-bridge Multilevel Inverters

Multilevel inverters are power electronic systems that synthesizes a desired output voltage from several levels of dc voltages as inputs. The term multilevel starts with the three-level inverter introduced by Nabae et al. [1] with an increasing number of dc voltage sources, the converter output voltage waveform approaches a nearly sinusoidal waveform while using a fundamental frequency-switching scheme. In order to do that, multilevel inverters include an array of power semiconductors and capacitor voltage sources, the output of which generate voltages with stepped waveforms. Some of the most attractive features discussed in the literature reviewed [2] about of multilevel inverters are as follows:

- They can generate output voltages with extremely low distortion and lower .
- They draw input current with very low distortion.
- They can operate with a lower switching frequency.

In this chapter, special attention is focused on the main features of multilevel cascaded H-bridge inverter, different kind of modulation techniques based on carrier based PWM such as: phase-shifted and level-shifted modulations are analyzed and their performance is compared.

4.1 Single Phase H-bridge Cells

Cascaded H-bridge multilevel inverter is composed of a multiple units of single phase H-bridge power cells as shown in fig 4.1. These cells are normally connected in cascade on their ac side. In practice, the number of power cells in a CHB inverter is mainly determined by its operating voltage and manufacturing cost. This kind of topology requires a number of isolated dc supplies, each of which feeds an H-bridge power cell. The dc supplies are normally obtained from multipulse diode rectifiers. For the five, seven and nine-level inverters, 12, 18 and 24 pulse diode rectifiers can be employed respectively.

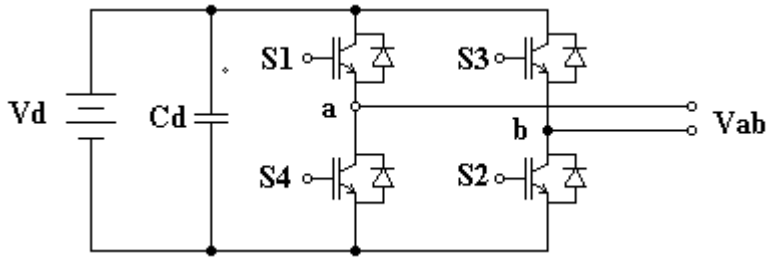

Figure 4.1 Single phase H-bridge inverter

One of the advantages of this topology is the ability to synthesize higher number of output voltage levels with an excellent harmonic spectrum using low cost and low voltage power semiconductors and capacitors. However, drawbacks of this topology are the large number of power cell devices and of voltages required to supply each cell with a complex and expensive isolated transformer.

4.2 H-bridge Cascaded Topologies

As is known the H-bridge multilevel inverter uses different cells connected in series chain to produce high ac voltage with low distortion currents. The number of cells is chosen typically from 2 to 5, for the worldwide standard machine voltage 2,3kV to 7,2kV. For example for two power cells per phase, the circuit can produce five distinct phase voltage levels. There are several families of H-bridge cells with the same input voltage (460V,630V and 690V) that are able to produce (800V, 1100V and 1200V) line to line output voltages for rated currents ranging from 70A to 1000A [3]. Nowadays different kind of topologies based on H-bridge cascaded are available in the industry, those, are summarized in table 4.1.

Drive	Switching device	Power range	Manufacterer
Robicon (perfect harmony)	IGBT	0,3MVA-22MVA	Siemens
Tosvert- MV		0,5MVA - 6MVA	Toshiba
Innovation MV-GP type H		0,45MVA - 7,5MVA	General electric

Table 4.1 Summary of industrial drives based on H-bridge multilevel inverters

As an example for the Robicon Perfect harmony, in order to produce a 4,16kV, four cells in cascaded are used per phase, and to generate 6,6kV to 7,2kV, six power cells per phase, are connected in series. However a five level inverter (two cells per phase) is used as a prototype in the present work. It is shown in figure 4.2.

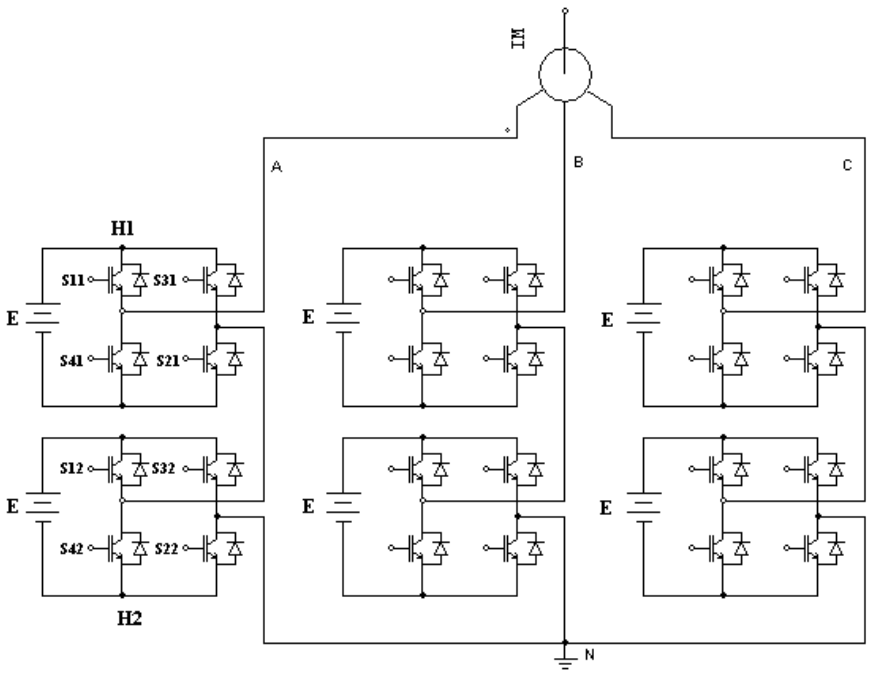

Figure 4.2 Five- level cascade H-bridge inverter

The cascade inverter in the figure above can produce a phase voltage with five voltage levels. The resultant inverter phase voltage is *UAN = UH1 + UH2*, which is the voltage at the inverter terminal A with respect to the inverter neutral *N*. The output voltage can be *0, ±E, ±2E*. The voltage levels which correspond to various switching states are summarized in table 4.2. It can be observed from the table that some voltage levels can be obtained by more than one switching state. These redundancies are common in multilevel inverters. It provides a great flexibility for switching pattern design, especially for space vector modulation schemes. In a general way If H is the number of single-phase H-bridges per phase, the number of levels of the inverter is:

$$m = (2H + 1) \tag{4-1}$$

The voltage level m is always an odd number for the Cascade H-bridge inverter while in other multilevel topologies such as diode-clamped inverters it can be either an even or odd number. This arrangement is called and Order-1 configuration [4].

There are other topologies of inverters where the dc supply of the H-bridge power cells is different. This allows more voltage steps in the inverter output voltage waveform for a given number of power cells. As an example, if the dc source in *H1 = E* and the dc source of *H2=2E*, the number of levels is seven (*3E,2E,E,0,-E,-2E,-3E*). There are some drawbacks with this kind of unequal H-bridge inverter and basically is about the difficulty to design the switching pattern due to the reduction in redundant switching states for space vector modulation. Therefore, this topology has limited industrial applications [5].

Output voltage	**Switching state**				**H1 cell voltage**	**H2 cell voltage**
U_{AN}	**S_{11}**	**S_{31}**	**S_{12}**	**S_{32}**	**U_{H1}**	**U_{H2}**
2E	1	0	1	0	E	E
E	1	0	1	1	E	0
	1	0	0	0	E	0
	1	1	1	0	0	E
	0	0	1	0	0	E
0	0	0	0	0	0	0
	0	0	1	1	0	0
	1	1	0	0	0	0
	1	1	1	1	0	0
	1	0	0	1	E	-E
	0	1	1	0	-E	E
-E	0	1	1	1	-E	0
	0	1	0	0	-E	0
	1	1	0	1	0	-E
	0	0	0	1	0	-E
-2E	0	1	0	1	-E	-E

Table 4.2 Voltage level and switching state of a five level cascaded H-bridge inverter

4.3 Modulation Techniques Based on Carrier Based PWM Schemes

The carrier-based modulation schemes for multilevel inverters can be generally classified into two categories: phase-shifted and level-shifted modulations. Both modulation schemes have been simulated and compared each other.

4.3.1 Phase Shifted Modulation

In general, a multilevel inverter with m voltage levels requires (*m–1*) triangular carriers. In this kind of modulation, all the triangular carriers have the same frequency and the same amplitude, but there is a phase shift between any two adjacent carrier waves, given by:

$$\varphi_{cr} = \frac{360^{\circ}}{m-1} \tag{4.2}$$

The gate signals are generated by comparing the modulating wave with the carrier waves. It means for the five level inverter, four are triangular carriers are needed with a 90° phase displacement between any two adjacent carriers. In this case the phase displacement of *Ucr1*=0°, *Ucr2*=90°, *Ucr1-* =180° *and Ucr2-* = 270°. As is shown in figure below:

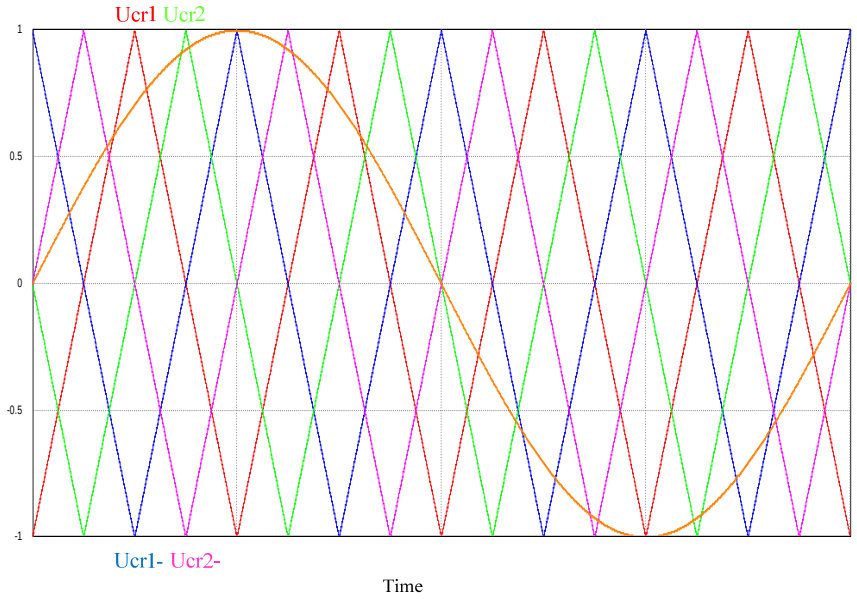

Figure 4.3 Modulating signal and triangular carriers base on phase shifted modulation

The logic to generate the gatings for the IGBTs by comparison of the modulating signal with the carrier waves, is described as follow: when the modulating signal (*Um*) is higher than the corresponding carrier *Ucr1* and *Ucr2* (used to generate gatings for the upper switches *S11* and *S12*), the switches *S11* and *S12* are turned on, in the left legs of power cells *H1* and *H2*, while when the modulating signal (*Um*) is lower than the carriers, *Ucr1–* and *Ucr2-* (which are 180° out of phase with *Ucr1* and *Ucr2*, respectively), produce the gatings for the upper switches *S31* and *S32*, in the right legs of the H-bridge cells. The gate signals for the lower switches in the H-bridge legs operate in a complementary manner with respect to their corresponding upper switches.

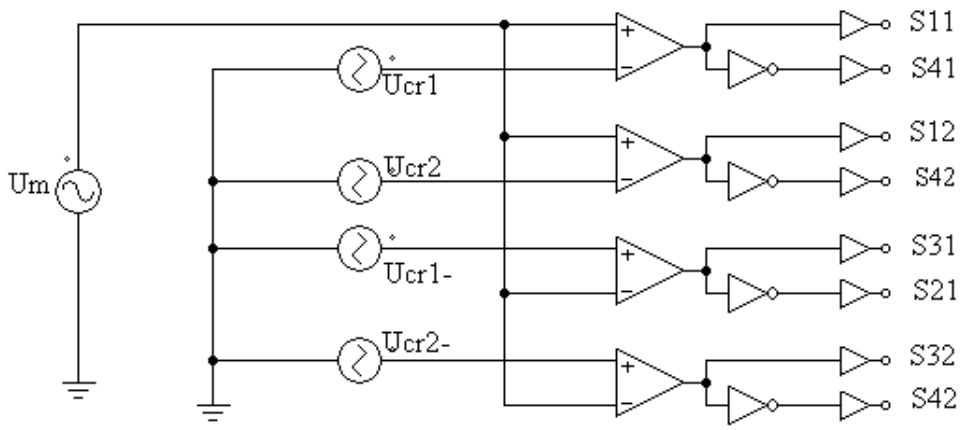

Figure 4.4 Logic to generate gating signals for IGBTs based on phase shifted modulation

The *H1* output voltage *UH1* is switched either between zero and *E* during the positive half-cycle or between zero and *-E* during the negative half cycle of the fundamental frequency. The frequency modulation index is given by the relationship between the frequency of the carrier frequency and the modulating signal ( )

$$mf = fcr/fm \tag{4-3}$$

The amplitude modulation index is given by:

$$ma = Um/Ucr \tag{4.4}$$

The frequency of the dominant harmonic in the inverter output voltage represents the inverter switching frequency f inv. In general, the switching frequency of the inverter using the phase-shifted modulation is given by:

$$finv = (m\text{-}1)\, fcr \tag{4-5}$$

The inverter switching frequency for a five level inverter, is given by *4fcr*, when the phase-shifted modulation is used. This is a desirable feature of the multilevel inverter since a high value of f inv allows more harmonics in *UAB* to be eliminated while a low value of *fcr* helps to reduce device switching losses. The maximum fundamental frequency voltage for ma = 1 can be found from [6].

$$UAB1,max = 0{,}612(m-1)E \tag{4-6}$$

4.3.2 Level Shifted Modulation

As same as the phase-shifted modulation, an m-level Cascaded H-bridge inverter using level-shifted modulation requires (*m–1*) triangular carriers, all having the same frequency and amplitude. The frequency modulation index is given by *mf = fcr/fm*, which remains the same as that for the phase-shifted modulation scheme whereas the amplitude modulation index is defined as:

$$m_a = \frac{Um}{Ucr(m-1)} \qquad \text{for} 0 \leq m_a \leq 1 \qquad (4\text{-}7)$$

where *Um* is the peak amplitude of the modulating wave and *Ucr* is the peak amplitude of each carrier. There are basically three types of schemes for the level-shifted modulation: (a) in-phase disposition (IPD), where all carriers are in phase; (b) alternative phase opposite disposition (APOD), where all carriers are alternatively in opposite disposition; and (c) phase opposite disposition (POD), see figure 4-5:

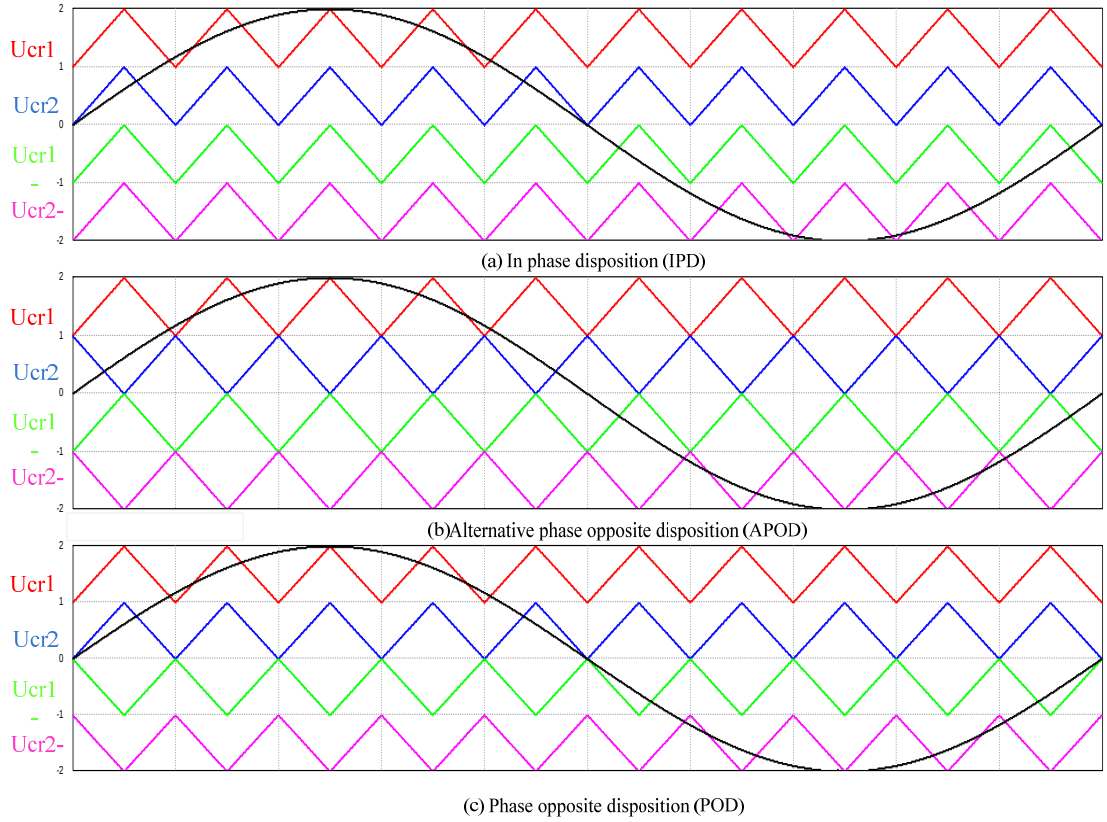

Figure 4.5 Level-shifted modulation for five level inverters a) In phase disposition, b) Alternative phase opposite disposition, c) Phase opposite disposition

The general logic of the level shifted modulation is described as follow: the uppermost and lowermost carrier pair, *Ucr1* and *Ucr1–,* is used to generate the gatings for switches *S11* and *S31* in power cell *H1* (see Fig. 4,2). The innermost carrier pair, *Ucr2* and *Ucr2–,* generate gatings for *S12* and *S32* in *H2*. For the carriers above the zero reference (*Ucr1* and *Ucr2*) the switches *S11* and *S12* are turned on when the modulating signal *Um* is higher than the corresponding carriers.

For the carriers Ucr1– and Ucr2– the switches S31 and S32 are turned on when Um is lower than the carrier waves. The gate signals for the lower switches in each H-bridge are complementary to their corresponding upper switches.

In general, the switching frequency of the inverter using the level-shifted modulation is equal to the carrier frequency, from which the average device switching frequency is

$$f_{sw} = \frac{f_{cr}}{m-1} \tag{4-8}$$

4.4 Comparison between Phase and Level-Shifted Modulation Methods

A comparison between the modulation techniques described above, is done based on the topology shown in fig 4.2. This H-bridge five level inverter is used as the case of study.

4.4.1 Phase Shifted Modulation Results

Normally the application of multilevel inverter is for high power application, where low frequency of carriers is required (around 600Hz [6]). In the present work, the multilevel inverter is used to control a 3kW, 460V induction motor with a subsea pump. Based on this theoretical work, the follow parameters are chosen in order to evaluate the performance of the modulation technique. Based on equation (4-6), a DC voltage of 190V is chosen in order to generate 460VLL. The main circuit is shown in appendix 2 and results are as follows:

Frequency of the modulating signal (*fm*)	50Hz
Peak amplitude of the modulating signal *(Um)*	1pu
Frequency of the carrier wave *(fcr)*	2,5kHZ
Peak amplitude of the carrier wave *(Ucr)*	1pu
DC voltage per H-bridge cell (*E*)	190V

Table 4.3 Parameters used for phase shifted modulation technique

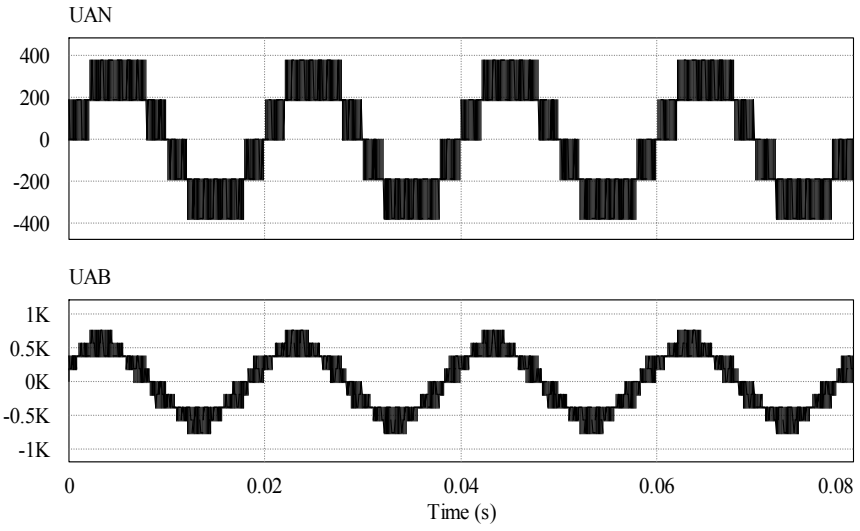

Figure 4.6 Waveforms of phase and line to line voltages of a phase A (Phase shifted modulation)

From the figure 4.6 can be seen the number of levels generated for the phase voltage (five levels) and for the line to line voltage (nine levels) as it was discussed before.

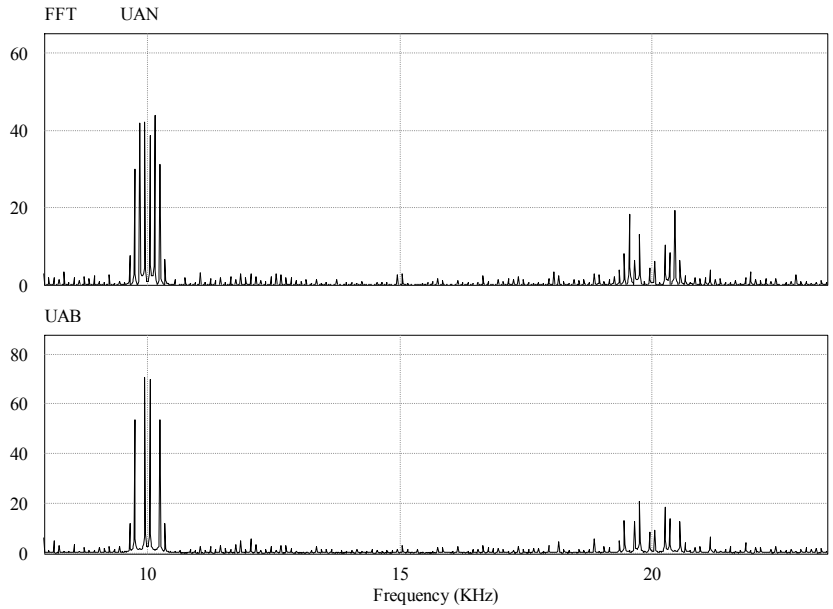

Figure 4.7 Harmonic spectrum of phase and line to line voltages of a phase A (Phase shifted modulation)

Since the dominant harmonics in UAB and UAN are distributed around 10kHZ and as stated earlier, the frequency of the dominant harmonic in the inverter output voltage represents the inverter switching frequency, it has demonstrated the equation (4-5) for phase shifted modulation. For the above spectrum and for a fundamental frequency of 50Hz, the THD obtained are 9,72% and 6,46% for the phase and line to line voltages respectively.

4.4.2 Level Shifted Modulation Results

The three different schemes for the level shifted modulation have been simulated and compare them in order to evaluate the content of harmonics. The parameters used are shown in table 4.4.

Frequency of the modulating signal wave (*fm*)	50Hz
Peak amplitude of the modulating wave *(Um)*	1pu
Frequency of the carrier wave *(fcr)*	10kHZ
Peak amplitude of the carrier wave *(Ucr)*	0.5 pu
DC voltage per H-bridge cell (*E*)	190V

Table 4.4 Parameters used for level shifted modulation technique

4.4.2.1 In Phase Disposition (IPD)

For the scheme based on phase disposition it has been found that the THD obtained are 6,51% and 3,19% for the phase and line to line voltages respectively. The five levels formed in the phase voltage and the nine levels formed in the line to line voltage is shown in figure 4.8. The harmonic spectrums of those voltages are shown in fig 4.9.

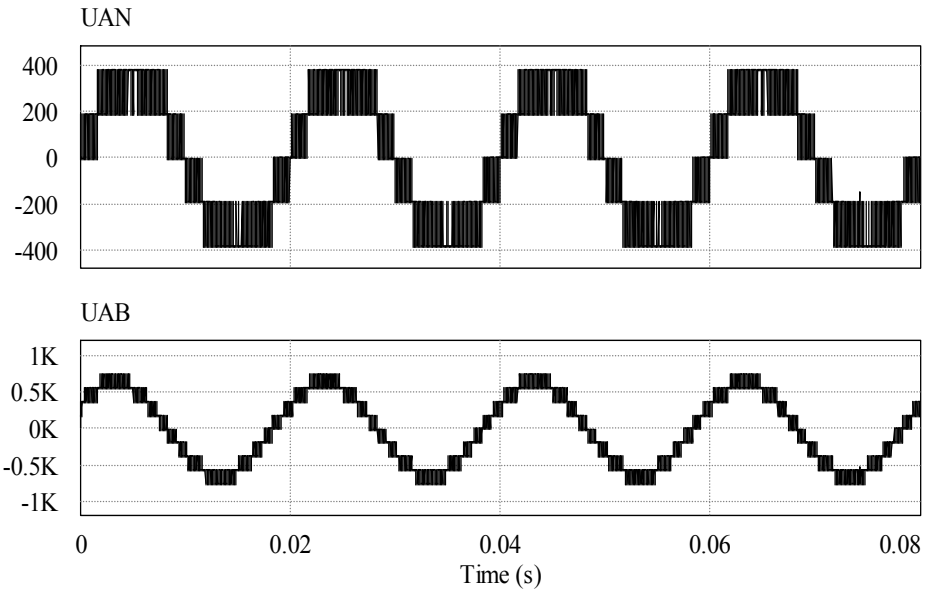

Figure 4.8 Waveforms of phase and line to line voltages of a phase A. Based on phase disposition (IPD)

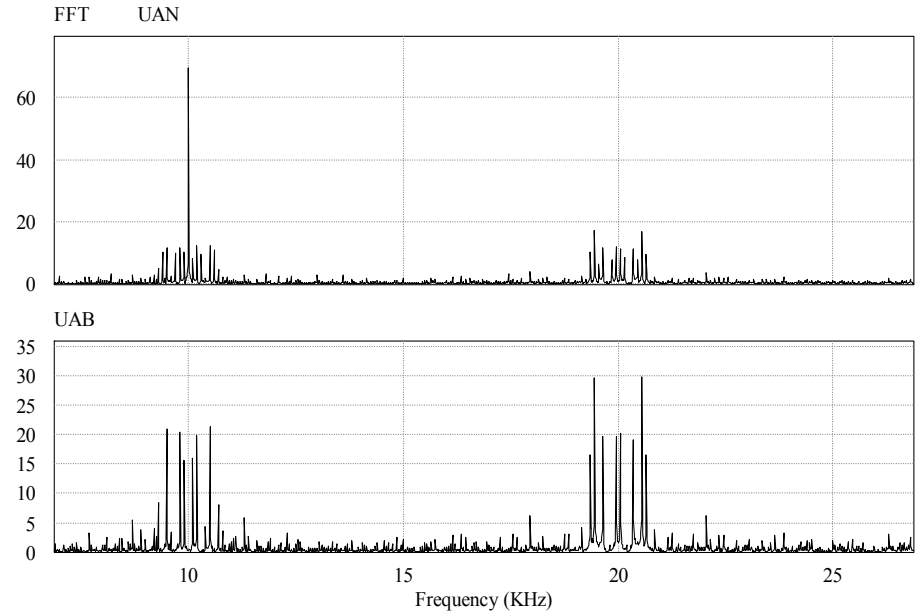

Figure 4.9 Harmonic spectrum of phase and line to line voltages of a phase A. Based on phase disposition scheme (IPD)

4.4.2.2 Phase Opposite Disposition (POD)

For the scheme based on phase opposite disposition it has been found that the THD obtained are 6,56% and 5,61% for the phase and line to line voltages respectively.

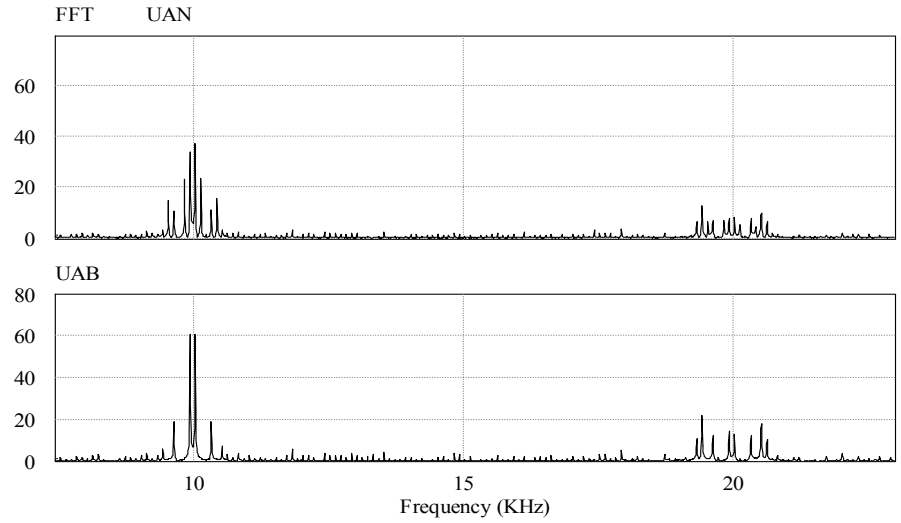

Figure 4.10 Harmonic spectrum of phase and line to line voltages of a phase A. Based on phase opposite disposition scheme (POD)

4.4.2.3 Alternative Phase Opposite Disposition (APOD)

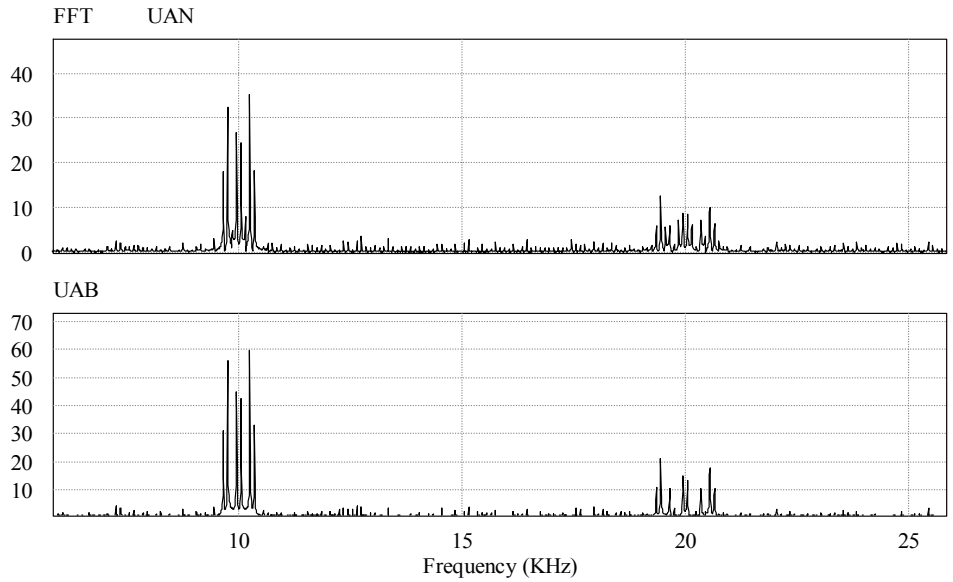

Figure 4.11 Harmonic spectrum of phase and line to line voltages of a phase A. Based on alternative phase opposite disposition scheme (APOD)

For the scheme based on alternative phase opposite disposition it has been found that the THD obtained are 5,68% and 5,61% for the phase and line to line voltages respectively.

One of the major adverse effects of harmonics are loses and pulsating torques in the induction motors, due to the importance of having less harmonic contents in the machine the THD is the main criteria to choose the modulation technique. In conclusion, it can be said that level phase shifted modulation produces a lower THD profile of the line to line voltage than phase shifted modulation, and within the different schemes analyzed above, in phase disposition (IPD) presents the lowest THD of the line to line voltage. Although nowadays commercial versions of the H-bridge multilevel inverter use the phase shifted modulation [7], the IPD Level shifted modulation scheme is chosen in this work as the modulation technique for the multilevel inverter. Table 4.5 summarizes the quantities comparison for H-bridge multilevel inverter with different H-bridge power cells per phase.

Number of H-Bridges per phase (H)	2	3	4	H
Number of phase output voltage level (n)	5	7	9	2H+1
Number of line to line output voltage level (N)	9	13	17	4H+1
Number of carrier signals	4	6	8	2H
Carrier phase shift displacement	90°	60°	45°	180/H

Table 4.5 Quantities comparison of cascaded H-bridge topology

In the H-bridge multilevel inverter the number of H-bridge cells per phase is primarily determined by the inverter operating voltage, harmonic requirements, and manufacturing cost. Multilevel inverters with seven to eleven voltage levels has been increasingly used in high-power medium-voltage (MV) drives, where the IGBTs are exclusively used as switching devices. However In the present work, a five level H-bridge cascaded with IPD level shifted modulation and switching frequency of 10 kHZ is chosen for the theoretical application of a subsea pump. Some features and drawbacks of this kind of topology including:

It does not require clamping diodes or voltage balancing capacitors, which are required in the NPC and the FLC topologies. The number of output voltage levels can then be easily adjusted by changing the number of H-bridge cells. Moreover, redundancy can be easily applied to enhance the reliability of the entire system. However, the control complexity is directly proportional to the number of H-bridge cells. As the number of voltage levels increases, the voltage imbalance problem becomes more of a concern. It needs a number of isolated dc supplies which are usually obtained from a multipulse diode rectifier employing an expensive phase shifting transformer.

4.5 References

[1]. Nabae, I. Takahashi, and H. Akagi, "A new neutral-point clamped PWM inverter," IEEE Trans. Ind. Applicat., vol. IA-17, pp. 518–523, Sept./Oct. 1981.

[2]. J. Rodriguez, J.S. Lai, F.Zheng. "Multilevel Inverters: A survey of Topologies, controls, and applications" IEEE Transactions on Industrial electronic, Vol 49. No 4. August 2002. pp 724-738.

[3]. S. Saeed Fazel, "Investigation and comparison of multi-level converters for medium voltage applications" Doctoral thesis, von der Fakultät IV- Elektrotechnik und Informatik der Technische Universität Berlin, Berlin 2007.

[4]. J.W. Bates: "Sequenced amplitude modulated inverters", IEEE-PESC'73 conference record, pp. 222-229.1973.

[5]. R.Lund "Multilevel power electronic converters for electrical motor drives" Doctoral thesis at NTNU 2005:62.Trondheim April 2005.pp 19.

[6]. Bin Wu, "High-Power converters and AC drives" ISBN: 9780471731719 , DOI:10.1002/0471773719 Copyright © 2006 the Institute of Electrical and Electronics Engineers, Inc.

[7]. P. Correa, M. Pacas, J. Rodriguez. "Predictive Torque control for Inverter-Fed Induction Machines" IEEE Transactions on Industrial Electronics, Vol 54,No 2, April 2007 pp. 1073-1079.

5. Control Strategies of Induction Motor Drives

Two control schemes, field-oriented control (FOC) and direct torque control (DTC), have become the industrial standards in high-power medium-voltage (MV) drives. This chapter focuses on FOC and DTC schemes for induction motor drives. The chapter starts with the dynamic models of the induction motor, follow by the emphasis of the flux oriented control scheme and a modified direct torque control based on PWM modulation.

5.1 Dynamic Model of the Induction Motor

Basically two commonly dynamic models for the induction motor are used. One is based on space vector theory and the other is based on *dq*-axis transformation. The space vector model features compact mathematical expressions and concise space vector diagram, whereas the *dq*-axis model does not need to use complex numbers or variables. Both models are valid for the analysis of transient and steady state performance of the induction motor.

5.1.1 Space Vector Induction Motor Model

In order to analyze the induction machine, it is assumed the induction motor is three-phase symmetrical and its magnetic core is linear with a negligible core loss. An induction machine is characterized by the following equations in a reference frame, rotating with the speed ω[2]:

$$\left.\begin{aligned} U_s &= R_s i_s + p\varphi_s + j\omega\varphi_s \\ U_r &= R_r i_r + p\varphi_r + j(\omega - \omega_r)\varphi_s \end{aligned}\right\} \tag{5.1}$$

From the above equations, Us and Ur are the stator and rotor voltage vectors, respectively, i_s and i_r are the stator and rotor current vectors, respectively, φ_s and φ_r are the complex notation of the stator and rotor flux linkages, respectively, Rs, Rr are the stator and rotor winding resistance, respectively, ω is the rotating speed of an arbitrary reference frame; ω_r is the rotor angular electrical speed. The flux linkage equations are given by:

$$\left.\begin{aligned} \varphi_s &= L_s i_s + L_m i_r \\ \varphi_r &= L_r i_r + L_m i_s \end{aligned}\right\} \tag{5.2}$$

where $L_s = L_{ls} + L_m$ and $L_r = L_{lr} + L_m$ represents the stator self-inductance and rotor self-inductance respectively, L_{ls}, L_{lr} and L_m are the stator, rotor leakage inductances and the magnetizing inductance respectively. The representation of the above equations is shown below:

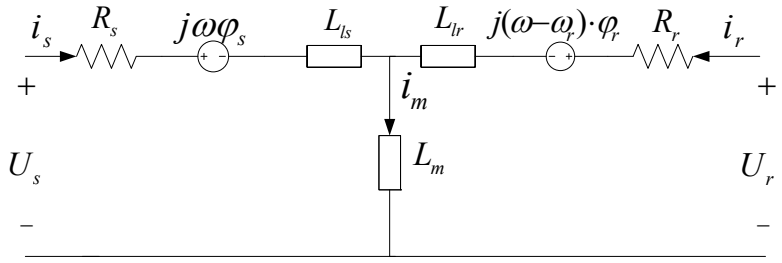

Figure 5.1 Space vector model of an induction motor

In order to describe the mechanical behavior of an induction motor, the following equations are valid:

$$\left.\begin{aligned} \frac{J}{P}p\omega_r &= T_e - T_L \\ T_e = \frac{3P}{2}Re(j\varphi_s {i_s}^*) &= \frac{3P}{2}Re(j\varphi_r {i_r}^*) \end{aligned}\right\} \tag{5-3}$$

From the above equations J is the inertia of the rotor and load, P is the number of pole pairs, *TL* is the load torque, and Te is the electromagnetic torque.

5.1.2 dq-Axis Motor Model

The induction motor dq-axis model can be derived using three-phase circuit theory and then transformed into the two-phase (dq-axis) frame [1]. Alternatively, it can also be obtained by decomposing the space vectors into the d- and q-axis components [2], as follow:

$$\begin{aligned} U_s &= U_{ds} + jU_{qs} & i_s &= i_{ds} + ji_{qs} & \varphi_s &= \varphi_{ds} + j\varphi_{qs} \\ U_r &= U_{dr} + jU_{qr} & i_r &= i_{dr} + ji_{qr} & \varphi_r &= \varphi_{dr} + j\varphi_{qr} \end{aligned} \tag{5.4}$$

Substituting (5-4) in (5-1) the dq-axis voltage equations for the stator and rotor if the induction motor can be obtained:

$$\left.\begin{aligned} U_{ds} &= R_s i_{ds} + p\varphi_{ds} - \omega\varphi_{qs} \\ U_{qs} &= R_s i_{qs} + p\varphi_{qs} - \omega\varphi_{ds} \\ U_{dr} &= R_r i_{dr} + p\varphi_{dr} - (\omega-\omega_r)\varphi_{dr} \\ U_{qr} &= R_r i_{qr} + p\varphi_{qr} + (\omega-\omega_r)\varphi_{dr} \end{aligned}\right\} \tag{5.5}$$

Replacing (5-4) in (5-2) the stator and rotor flux-linkages can be obtained by:

$$\left.\begin{aligned}\varphi_{ds} &= L_{ls}i_{ds} + L_m(i_{ds} + i_{dr})\\ \varphi_{qs} &= L_{ls}i_{qs} + L_m(i_{qs} + i_{qr})\\ \varphi_{dr} &= L_{lr}i_{dr} + L_m(i_{ds} + i_{dr})\\ \varphi_{qr} &= L_{lr}i_{qr} + L_m(i_{qs} + i_{qr})\end{aligned}\right\} \quad (5\text{-}6)$$

Normally the electromagnetic torque can be expressed as:

$$T_e = \frac{3}{2}P(i_{qs}\varphi_{ds} - i_{ds}\varphi_{qs}) \quad (5\text{-}7)$$

5.2 Field Oriented Control (FOC)

This method was developed around 40 years ago. In 1971 F. Blaschke [2] presented the first paper on field-oriented control (FOC) for induction motors. Since that time, the technique was completely developed and today is mature from the industrial point of view. Today field oriented controlled drives are an industrial reality and are available on the market by several producers and with different solutions and performance [3]. Basically the method demonstrates that an induction machine can be controlled like a separately excited dc motor. This means there is a decoupling effect between the torque and the flux with an excellent dynamic performance.

5.2.1 Principle of Operation

In a dc machine, neglecting the armature reaction effect and field saturation, the developed torque is given by:

$$T_e = K_a\varphi_f i_a \quad (5\text{-}8)$$

Where K_a is an armature constant, i_a is the armature current, φ_f is the flux produced by the field current. In high performance dc drives, φ_f is perpendicular to the flux produced by the armature current i_a . These space vectors are orthogonal and decoupled in nature. It means that when φ_f remains constant by keeping constant the field current i_f, the torque can be directly controlled by i_a. The control of induction motors can be done based on the dc drives control. Using a proper field orientation, the stator flux can be decomposed into a flux-component and torque-component. These two components can be controlled independently. There field oriented control can be implemented based on the orientation of the stator flux, air gap flux and rotor flux. The orientation of the rotor flux has been used widely because of it gives natural decoupling control, while decoupling compensation currents have to be used when the stator flux or air gap used are orientated [4]. In this work the control is developed based on the rotor flux orientation.

5.2.2 Rotor Flux Orientation

The correct rotor flux orientation of the rotor flux vector φ_r is achieved by the alignment of d-axis frame, which is rotating at synchronous speed with respect to stationary frame, as is shown in figure 5.2.

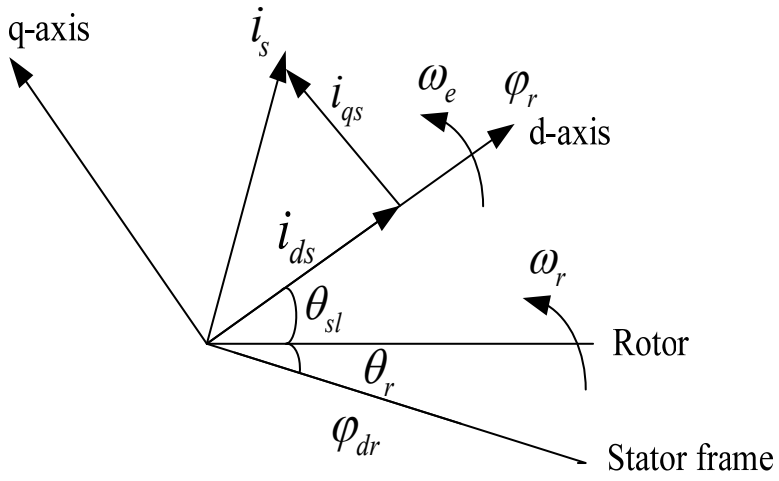

Figure 5.2 Rotor flux field orientation

5.2.3 Methods Based on FOC

In an induction machine the rotor speed is not equal to the rotor flux speed (there is a slip speed), then it is necessary a method to calculate the rotor flux angle θ_f. Several schemes have been proposed to find it, due this, the field orientation method can be classified into direct and indirect field oriented controls. If the rotor flux angle θ_f is calculated using the measured of the terminal voltages and currents, the method is direct field-oriented control. If the rotor flux angle θ is obtained from detected rotor position angle θ_r and calculated the slip angle θ_{sl}, the method is known as indirect field oriented control [5]. In this work an indirect field oriented control has been used to control a subsea pump. The method is described below

5.2.3.1 Indirect Field Oriented Control

A speed sensor (encoder) is required in the method. The rotor flux angle θ_{sl} is obtained from the measured rotor speed ω_r and from the calculation of the slip angle ω_{sl} based on the parameters of the machine. A typical scheme of the indirect FOC is shown in figure 5.3.

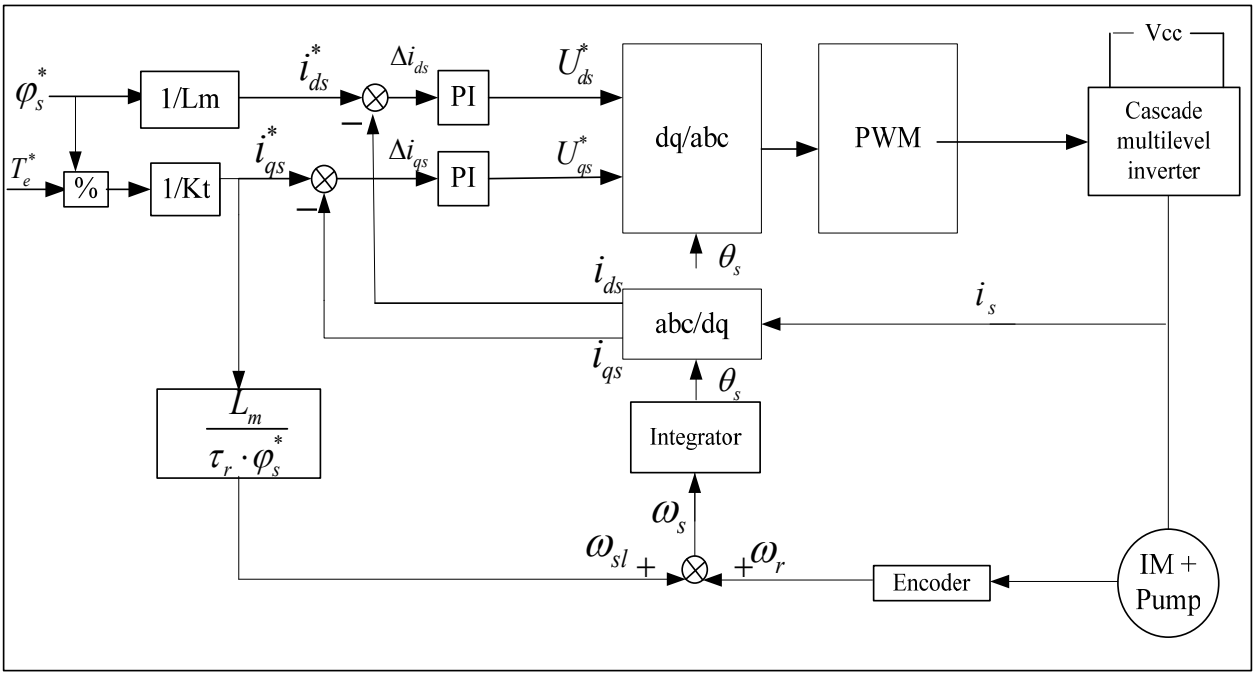

Figure 5.3 Indirect field oriented control with rotor flux orientation

Since the rotor speed ω_r is directly obtained, the rotor flux angle θ_s can be found as:

$$\theta_s = \int (\omega_r + \omega_{sl})\, dt \tag{5-9}$$

The slip frequency ω_{sl} can be derived from the synchronous frame motor model, where:

$$p\varphi_r = -R_r i_r - j\omega_{sl}\varphi_r \tag{5-10}$$

The rotor current is given by:

$$i_r = \frac{1}{L_r}(\varphi_r - L_m i_s) \tag{5-11}$$

Replacing (5.11) in (5.10):

$$p\varphi_r = -\frac{R_r}{L_r}(\varphi_r - L_m i_s) - j\omega_{sl}\varphi_r \tag{5-12}$$

Defining the rotor time constant τ as:

$$\tau = \frac{L_r}{R_r} \tag{5-13}$$

Writing (5-12) into dq-axis components and taking into account the rotor flux orientation $(j\varphi_{qr} = 0)$ and $(\varphi_{dr} = \varphi_r)$ the next equations are obtained:

$$\left.\begin{aligned} \varphi_r(1+p\tau_r) &= L_m i_{ds} \\ \omega_{sl}\tau_r\varphi_r &= L_m i_{qs} \\ \omega_{sl} &= \frac{L_m}{\tau_r\varphi_r} i_{qs} \end{aligned}\right\} \quad (5.14)$$

Normally during operation $\varphi^*{}_r$ is kept constant during operation ($p\varphi^*{}_r = 0$) therefore, $i^*{}_{ds}$ can be expressed as:

$$i^*{}_{ds} = \frac{1}{L_m}\varphi^*{}_r \quad (5.15)$$

The q-axis current reference can be written from the torque equation (5-8) as:

$$i^*{}_{qs} = \frac{1}{K_T\varphi^*{}_r} T^*{}_e \quad (5\text{-}16)$$

From (5-16) can be said that for a given $\varphi^*{}_r$ the torque producing current is proportional to $T^*{}_e$.

5.3 Direct Torque Control (DTC)

In the mid-1980s a technique for the torque control of induction motors was developed and presented by I. Takahashi as direct torque control (DTC) [5]. Since the beginning, the new technique was characterized by simplicity, good performance and robustness. Using DTC it is possible to obtain a good dynamic control of the torque without any mechanical transducers on the machine shaft. Thus, DTC can be considered as "sensorless type" control techniques. Different schemes have been developed based on the DTC principle. The classical method and a modified version of DTC is shown in the present work.

5.3.1 Principle of Direct Torque Control

One of the ways to express the torque developed by an induction motor is shown in equation (5-17):

$$T_e = \frac{3P}{2}\frac{L_m}{\sigma L_s L_r}\varphi_s\varphi_r sin\theta_T \quad (5\text{-}17)$$

Where θ_T is the angle between the stator flux vector and the rotor flux vector, called torque angle. Therefore the torque can be controlled by using this angle. The main variable controlled in DTC is the stator flux vector φ_s, it relates the stator voltage U_s by:

$$p\varphi_s = U_s - R_s i_s \quad (5\text{-}18)$$

The equation shows that the stator flux reacts to changes in the stator voltage, which is the same as the inverter output voltage. The method is based on controlling that voltage using a reference voltage in the space vector modulation. Since the reference voltage is synthesized by the stationary voltage vectors of the inverter, a proper selection of the stationary vectors can make the magnitude and angle of the stator flux adjustable.

Figure 5.4 shows a typical scheme based on direct torque control, as same as FOC, the method controls the flux and torque separately. The stator flux reference and torque reference are compared with the estimated values of flux and torque respectively. Those errors are sent to hysteresis comparators. The outputs of the comparators are sent to switching logic unit for proper selection of the voltage vectors (switching states) of the inverter.

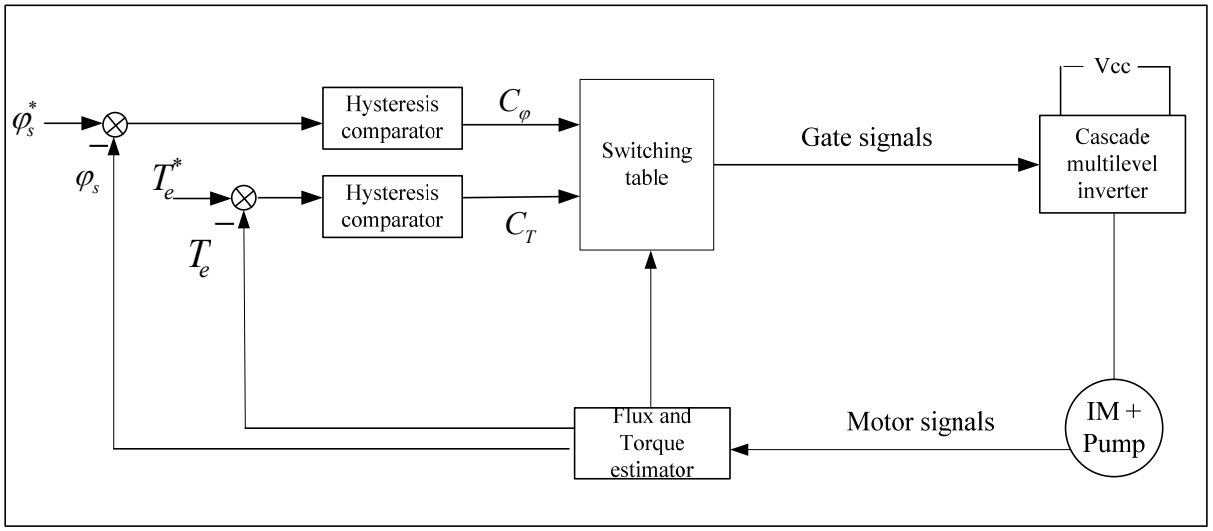

Figure 5.4 Classic Direct torque control scheme

Both comparators are hysteresis type, whose transfer characteristics are shown in figure 5.5. The flux comparator has two levels (+1,-1) while the torque comparator has three levels (+1,0,-1), where +1 means that a increase in φ_s or θ_T is required. -1 demands a decrease in φ_s or θ_T, while 0 means no changes.

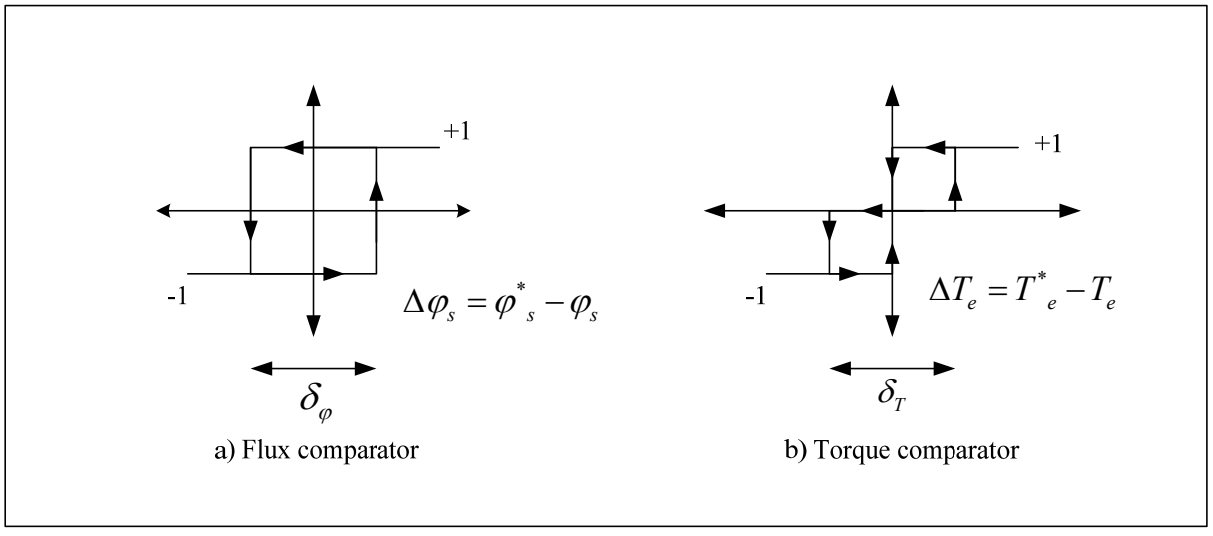

Figure 5.5 Characteristics of hysteresis comparators

The inputs of the switching table are the outputs of the comparators and the sector number (it depends of the number of levels of the multilevel inverter). The output of the comparators decide which voltage vector should be chosen.

5.3.1.1 Modified Direct Torque Control

In the classical DTC algorithm, the decoupling of nonlinear AC motor characteristics is achieved by the on-off operation of the hysteresis controller. However, the number of switching states of multilevel inverters is M^3 (where M is the level number of multilevel inverters). For example, for a five level inverter, there are 125 switching states. Of course there are some redundancies states, but the switching table is still difficult to form. In [6] the hysteresis PWM controller has been replaced by space vector modulation (SVM) in DTC to make torque response smooth and switching frequency fixed. In according with the literature review, the main issues of traditional DTC are the large torque ripples and unfixed switching frequency [7]. In order to avoid these problems, space vector modulation has been adopted to DTC method. In this work the DTC implemented is based on the modified version described above but it has been implemented instead of space vector modulation, PWM carrier modulation.

In according with [6], the use of space vector modulation with DTC produces an improvement performance of the speed control of high-voltage motors, a reduction of the harmonic content of output voltage and current, and the torque ripple can also be further lighten.

The modified DTC scheme is shown in figure 5.6. Here the hysteresis comparators have been replaced by PI controllers.

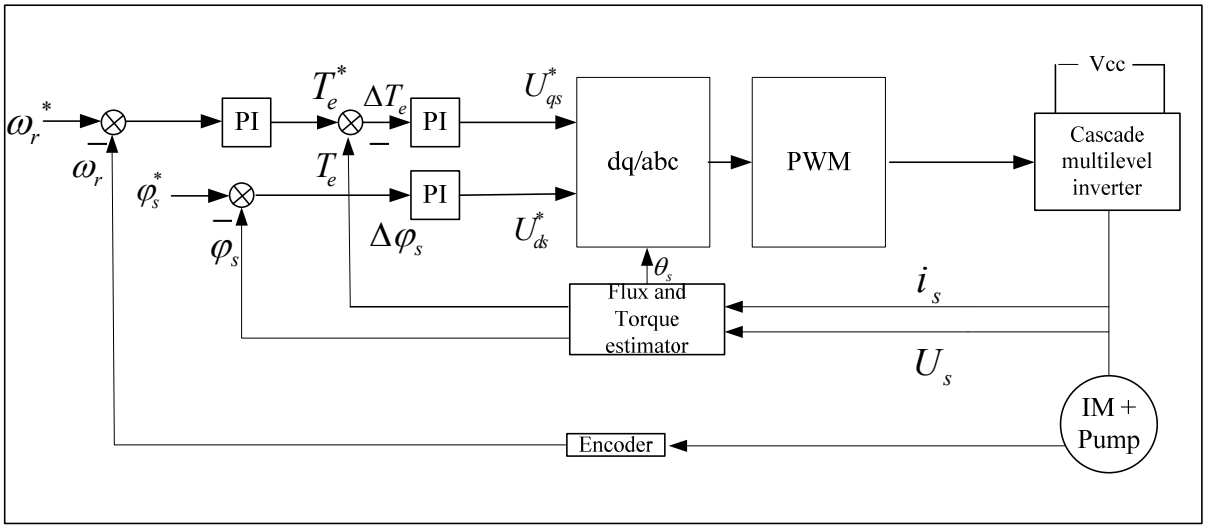

Figure 5.6 Scheme diagram of DTC for conventional carrier PWM

In the scheme diagram shown above, the observation model to estimate the torque and flux is same as classic DTC. After the calculation of the flux error and torque error, as for how to decide the desired voltage vector by them, several effective strategies have been proposed [9]. The scheme of using two PI controllers (one for flux and one for torque) to derive the inverter's command signals ($U_{d,}U_q$) has been adopted in this work, and its principle is illustrated below.

The *dq* components of the reference voltage vector in a stator flux reference frame are given by:

$$U_{sd}^{*} = \left(K_{p\varphi} + \frac{K_{I\varphi}}{s}\right)\Delta\varphi_s \tag{5-19}$$

$$U_{sq}^{*} = \left(K_{pT} + \frac{K_{IT}}{s}\right)\Delta T_e + \varphi_s\omega_{\varphi s} \tag{5-20}$$

The stator flux can be estimated from equation (5-18) by:

$$\varphi_s = \int_0^t (U_s - R_s i_s)dt \tag{5-21}$$

The flux variation in a sample time is given by:

$$\Delta\varphi_s = (U_s - R_s i_s)T_s \tag{5-22}$$

In a stationary reference frame and from two successive estimations of the stator flux:

$$\varphi_s(n+1) - \varphi_s(n) = (U_s(n) - R_s i_s)T_s \tag{5-23}$$

At high speed, the voltage drop ($R_s i_s$) can be neglected and the voltage becomes proportional with the flux change and with the switching frequency 1/Ts [8]. Therefore the equation is obtained as:

$$\Delta\varphi_s = |\varphi_s(n+1)| - |\varphi_s(n)| \approx U_d T_s \tag{5-24}$$

For each sampling period *Ts*, one can approximate the voltage as:

$$U_d = \frac{\Delta\varphi_s}{T_s} \tag{5-25}$$

If the stator flux is constant, the torque can be controlled by the imaginary component U_q

$$U_q T_s = |\varphi_s(n+1)|\sin(\Delta\theta) \approx |\varphi_s(n+1)|\Delta\theta \approx \varphi_s^{*}\Delta\theta \tag{5-26}$$

where is obtained:

$$U_q = \frac{\Delta\theta}{T_s}\varphi_s^{*} = \omega_e\varphi_s^{*} \tag{5-27}$$

One of the ways to express the relationship of the electric torque and flux is given by:

$$T_e = \frac{3}{2}\frac{p}{L_s}(\varphi_r \times \varphi_s) \tag{5-28}$$

The equation (5-28) shows that the control of the electric torque can be done by changing the angle between stator flux and rotor flux under the condition of their amplitudes are constant. Because of the large inertia of rotor, its flux cannot be changed suddenly [8].

Thus the electric torque can be regulated by changing the stator flux speed ω_e. The equation (5-27) shows that stator flux speed is decided by U_q, so the electric torque can be regulated by U_q.

With base on the modified DTC described above and from the above analysis, it can said that the amplitude of stator flux is decided by U_d, and the electric torque is decided by U_q, when the flux amplitude is constant. Using two PI controllers to regulate flux and electric torque respectively, the U_d and U_q, can be obtained in order to use them for either space vector modulation or PWM carrier modulation.

5.4 References

[1]. P. C. Krause, O. Wasynczuk, and S. D. "Sudhoff, Analysis of Electric Machines and Drive Systems", 2nd edition, Wiley-IEEE Press, New York, 2002.

[2]. F. Blaschke, "A new method for the structural decoupling of A.C. induction machines," in Conf. Rec. IFAC, Duesseldorf, Germany, Oct. 1971, pp. 1–15.

[3]. A. Nabae, K. Otsuka, H. Uchino, and R. Kurosawa, "An approach to flux control of induction motors operated with variable-frequency power supply," IEEE Trans. Indust. Applicat. Syst., vol. IAS-16, pp. 342–349, May/June 1980.

[4]. Bose, B. K. "Modern Power Electronics and AC Drives". Upper Saddle River, NJ: Prentice-Hall, 2002.

[5]. Bin Wu, "High-Power Converters and ac Drives" Print ISBN: 9780471731719 , DOI: 10.1002/0471773719 Copyright 2006 the Institute of Electrical and Electronics Engineers, Inc.

[6]. Y. Wang, H. Li, X. Shi "Direct Torque Control with Space Vector Modulation for Induction Motors Fed by Cascaded Multilevel Inverters" Key Laboratory of Power System Protection and Dynamic, North China Electric Power University.

[7]. Isao Takahashi, Toshihiko Noguchi, "A new quick response and high-efficiency control strategy of an induction motor", IEEE Trans Ind Appl, vol.IA-22, no.5, pp. 820-827, September-October, 1986.

[8]. C. Lascu, I. Boldea, F. Blaabjerg "A modified Direct torque control for Induction Motor Sensorlees Drive" IEEE Transactions on Industry Applications vol, 36 no 1, January/ February 2000, pp 122-130.

6. Modelling and Simulation Results

This chapter starts with an overview of the methods to implement current controllers needed to control AC drives. The main results obtained from the field oriented control and modified direct torque control and their respectively analysis are shown in detail.

6.1 Current Control

As is presented in chapter 5, field oriented control and direct torque control need an inner loop to control the current and generate the input references for the multilevel inverter. Several ways to implement those controllers can be mentioned as:

- Hysteresis control
- Stator frame PI controllers
- Synchronous frame PI controllers

6.1.1 Hysteresis Control

This method is based on the measure of the phase current and then subtracts it from its reference signal (a sinusoid). The error signal is then fed to a hysteresis comparator, the output of which forms the gate signal to the respective inverter leg. The method is shown in figure 6.1.

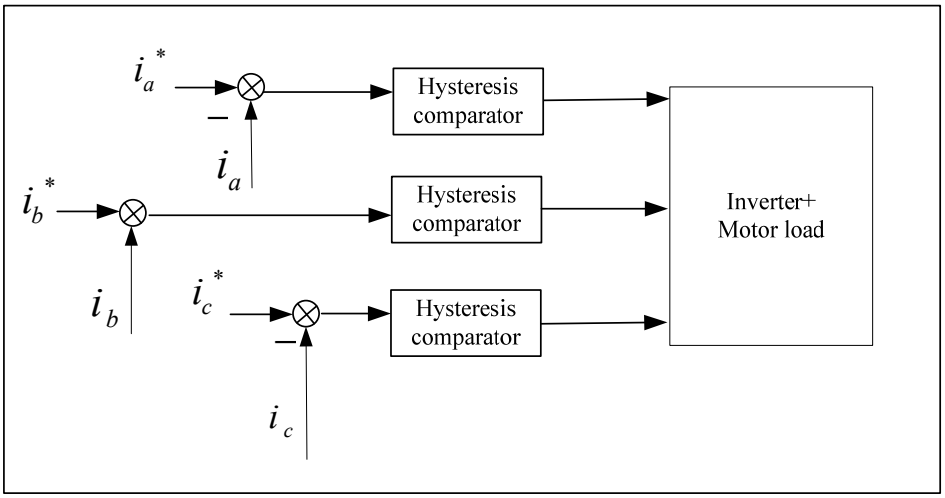

Figure 6.1 Hysteresis control

One of the advantages of this control method is that pulse width modulation (PWM) is made directly by the controller. Therefore no additional circuit or algorithm is required. The switching frequency is varied modifying the tolerance band of the hysteresis comparator. The difficulty of implementation in digital devices is one of the main drawbacks of this method [1].

6.1.2 Stator - Frame PI Control

For this scheme is common to use two standard PI controllers (one each for the α and β axes). The controller outputs are used as command signals to a PWM circuit. Unlike hysteresis control, this scheme uses two stages: control and modulation. One of the advantages of this scheme is that any PWM scheme can be employed. The drawback of this control scheme is that the actual current will not follow the reference in the steady state [2]. The control scheme is shown in figure 6.2.

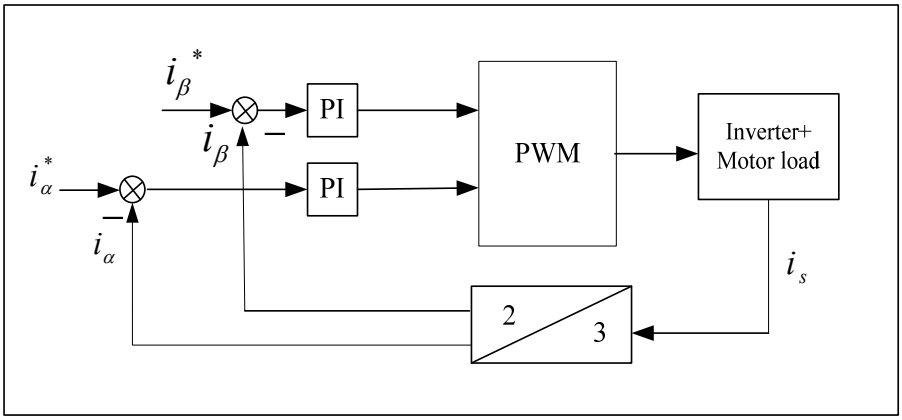

Figure 6.2 Stator-frame PI Control

6.1.3 Synchronous - Frame PI Control

The drawback of stator-frame PI control can be solved. The *αβ* sinusoidal signals can be *dq* transformed to the synchronously rotating reference frame, i.e. to DC signals in the steady-state, where standard PI control works properly. The coordinate transformation requires some multiplications and the calculation of sine and cosine of the transformation angle.

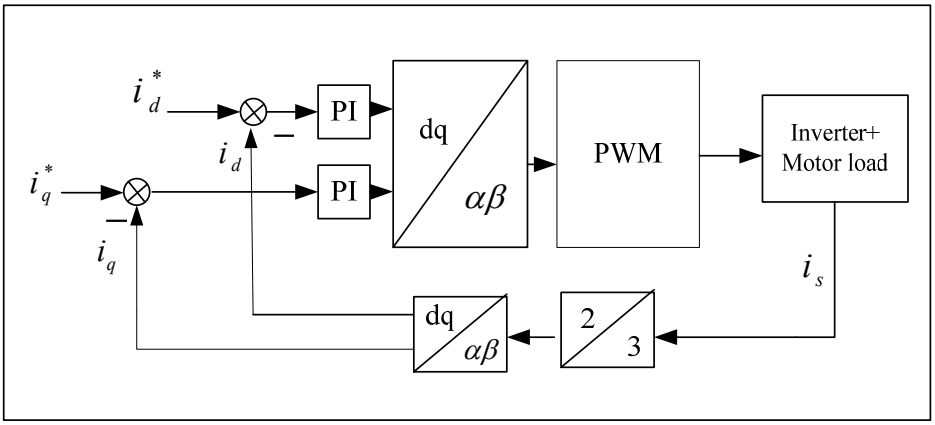

Figure 6.3 Synchronous-frame PI Control

Synchronous-frame PI controllers is the most attractive choice for current control, due to their simplicity and ability to provide satisfactorily good performance.

6.2 Indirect Field Oriented Control (IFOC)

The implementation of the indirect field oriented control scheme shown in figure 5.3 using PSIM is described in figure 6.4. Here synchronous frame PI controllers are implemented. Therefore, the stator current measurements are transformed to a synchronously rotating reference frame dq.

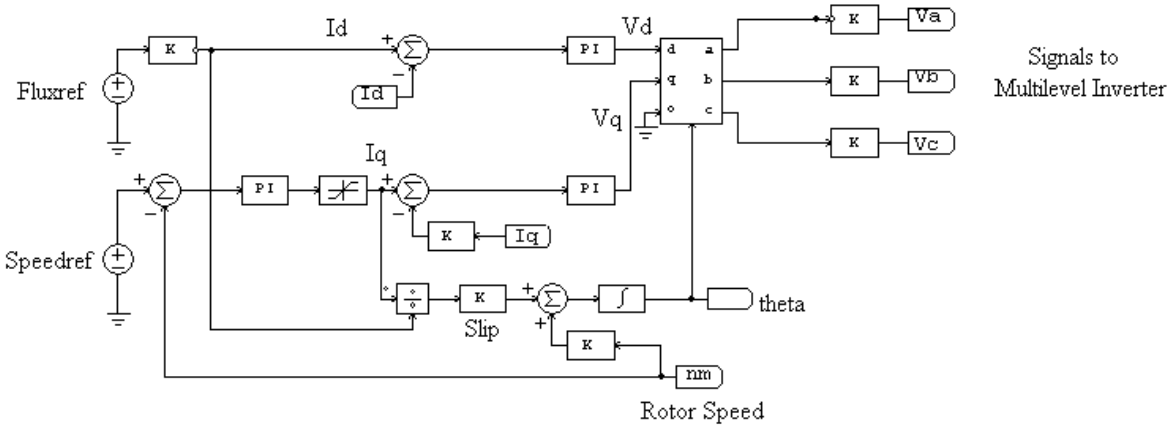

Figure 6.4 Indirect field oriented controller implemented in PSIM

Currents Id and Iq come from the park transformation of the stator currents. The reference flux used for the induction motor control is set to 0,65T. Therefore and in according with the equation (5-15), the current reference *Ids* is given by:

$$Ids=0,65T/0,041H=15,8A \quad (6\text{-}1)$$

From equation (5-13) the rotor time constant τ is defined by:

$$\tau=Lr/Rr=(0,74mH+41mH)/0,156\Omega = 0,26 \quad (6\text{-}2)$$

The angular slip frequency *ωsl* defined in (5-14) can be written using (5-15) as:

$$\omega sl= (1/\tau)\ (iqs/ids) =3,8(iqs/ids) \quad (6\text{-}3)$$

With *ωsl* as a known value and *ωr* in *rad/sec*, the rotor flux angle θs can be found from:

$$d\Theta s/dt= (\omega r+ \omega sl) \quad (6\text{-}4)$$

This angle is used to make the transformation of the stator currents to a synchronously rotating reference frame *dq*.

6.2.1 Speed Loop Controller

PI controllers have been used to adjust the system for desired responses. The tuning of the controller parameters (gain and time constant) is a compromise between speed of response and stability for small disturbances as well as the robustness to tolerate large signal disturbances. The function of the external PI controller used in the speed loop is to set the i_q reference. The gain settings of this controller have been made such that it stabilizes the speed error and gives fast speed response. Because of the electric dynamic of the machine is faster than the mechanical dynamic of the machine, the speed controller has to be slower than the inner control loop response. A trial and error method is used to find the gain and time constant of the controller. The procedure to set up the controller parameters is shown in appendix 3.

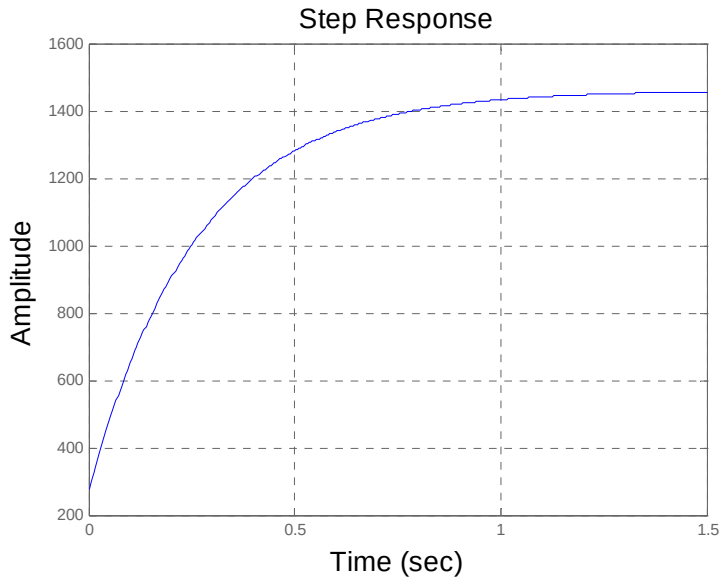

Figure 6.5 Step response of the speed controller

From figure 6.5, for a speed reference of 1400RPM, the steady state is reached at 1,5 sec. The value selected for the speed loop PI controller $K_p\left(1+\frac{1}{T_i}\right)$ is proportional gain (*Kp*) = 1 and time constant (*Ti*) = 0,05. A hysteresis band is used in the output of the speed control loop in order to limit the maximum electric torque developed during transient periods, this value is fixed in (-50, +50).

6.2.2 Inner Current Loop Controller

Here synchronous frame PI controllers are implemented. The PI controllers define the reference for *Ud* and *Uq* which are the inputs of the modulation technique. The machine is described by a first-order complex-valued system:

$$G(S) = \frac{1}{R+LS} \tag{6-5}$$

Where *G(S)* is the transient equivalent circuit transfer function, *R=Rs+Rr* and *L=Ls+Lr*. Therefore, the stator current loop with PI control is defined as figure 6.6:

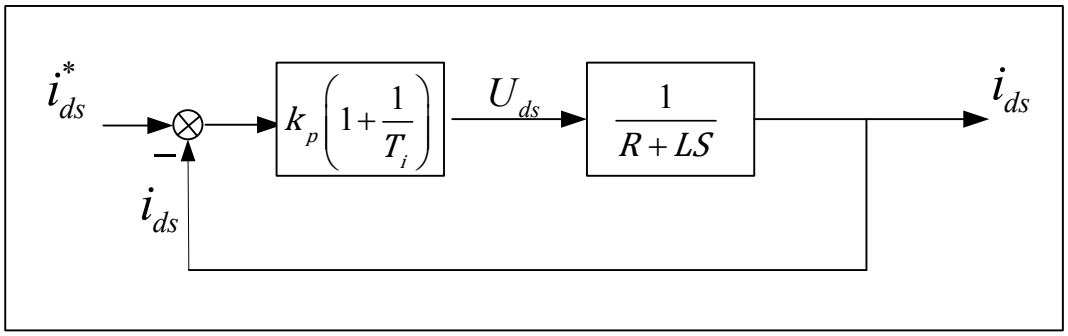

Figure 6.6 Inner current loop with PI control

A fast controller is necessary for the inner current loop. Generally the parameters of the PI controller are chosen by trial and error. A typical way to define the rise time is based on the switching frequency of the inverter as follow [3]:

$$f_{sw} \geq \frac{5\ln(9)}{2\pi t_r} = \frac{1{,}75}{t_r} \tag{6-6}$$

For a step input the rise time is chosen as 0,1s is suggested in [4]. It is clear that with a switching frequency of 10 kHZ the rise time fulfils the equation (6-6). Those parameters are found as: proportional gain (*Kp*) = 0.02 and time constant (*Ti*) = 0,001. Because of the inner Id current loop is the same as *Iq*. The parameters of the PI controllers are the same. Therefore, it is enough to set up the PI parameters for one of them.

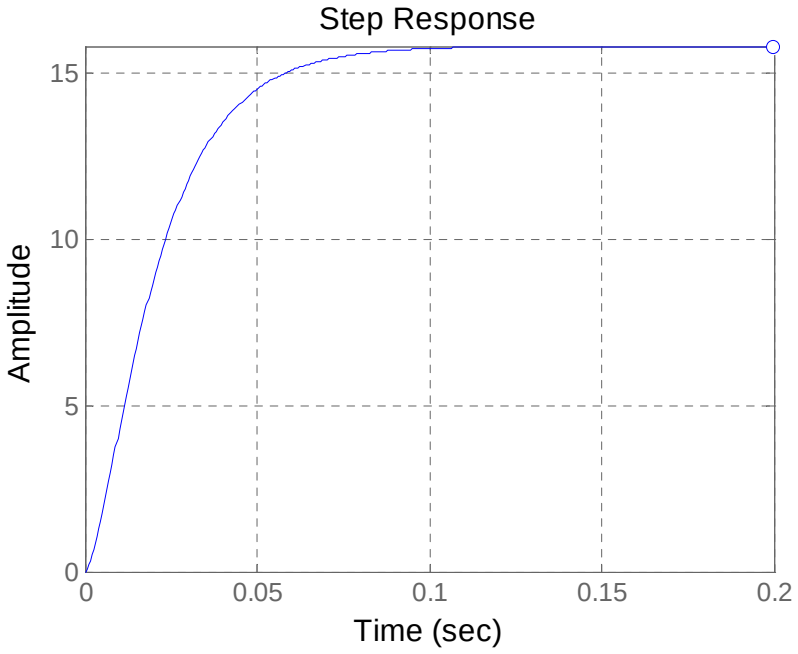

Figure 6.7 Step response of the inner current loop controller

Figure 6.7 shows the step response of both inner current loop controllers. The procedure to set up the PI parameters, it is shown in appendix 4.

6.2.3 Simulation Results

Indirect field oriented control has been carried out by numerical simulations using PSIM, this tool was chosen because of the high speed running simulations using drives. Based on the above parameters and numerical calculations described above, and with a variation of the load of 20Nm at 1sec the results are as follows:

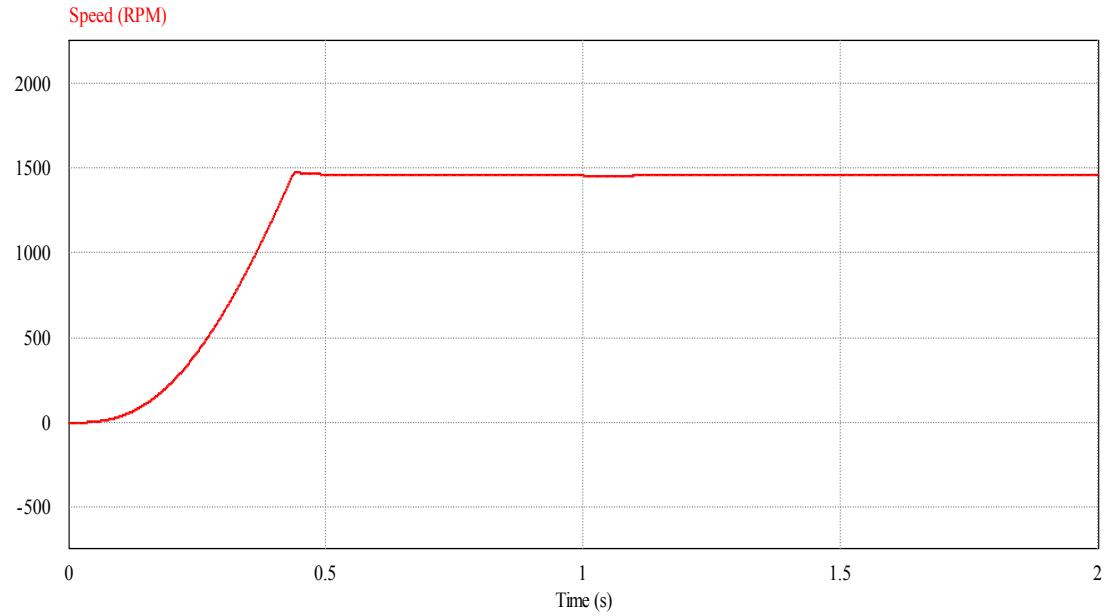

Figure 6.8 Speed response (rated speed=1460RPM) (IFOC)

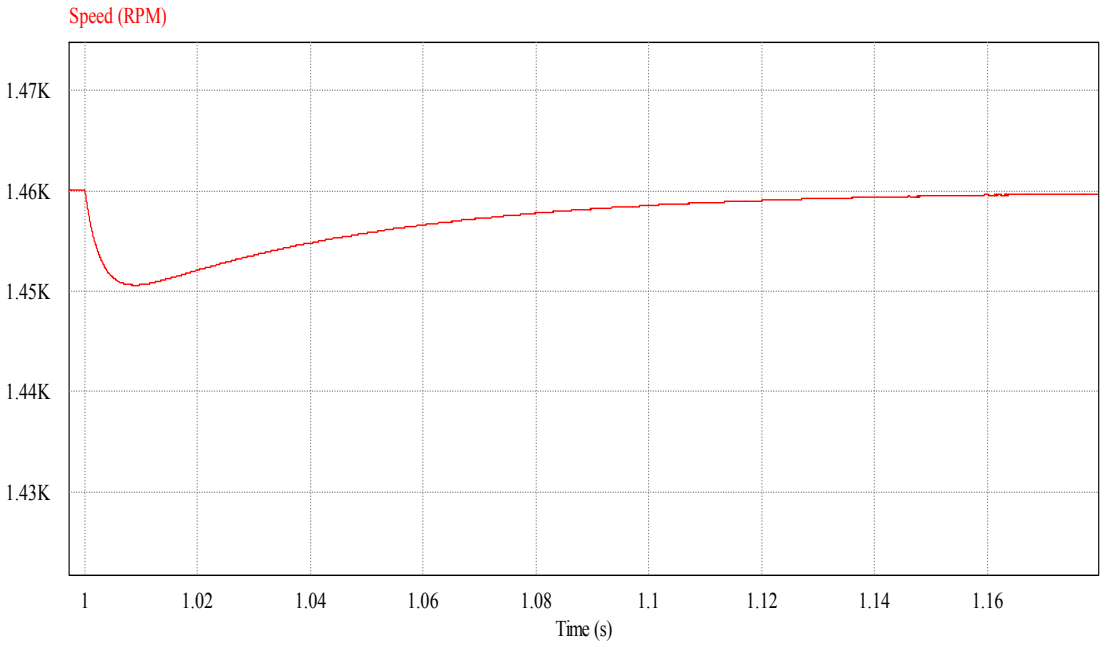

Figure 6.9 Speed variation at t=1 s when a load of 20Nm is connected (IFOC)

The machine initially operates at zero speed. The machine accelerates under no-load conditions until the rated speed of 1460RPM is reached at 0,45 s as is shown in figure 6.7. A load of 20Nm is connected to the machine at time instant of 1 s and the speed drops to 1450 RPM. The controller takes 0,16 s to recover the speed to the rated value (see figure 6.9).

The variations of the mechanical torque can be understood as variation of the volume of oil during the operation of the subsea pump. In this case and increasing of in the load of 20Nm is considered.

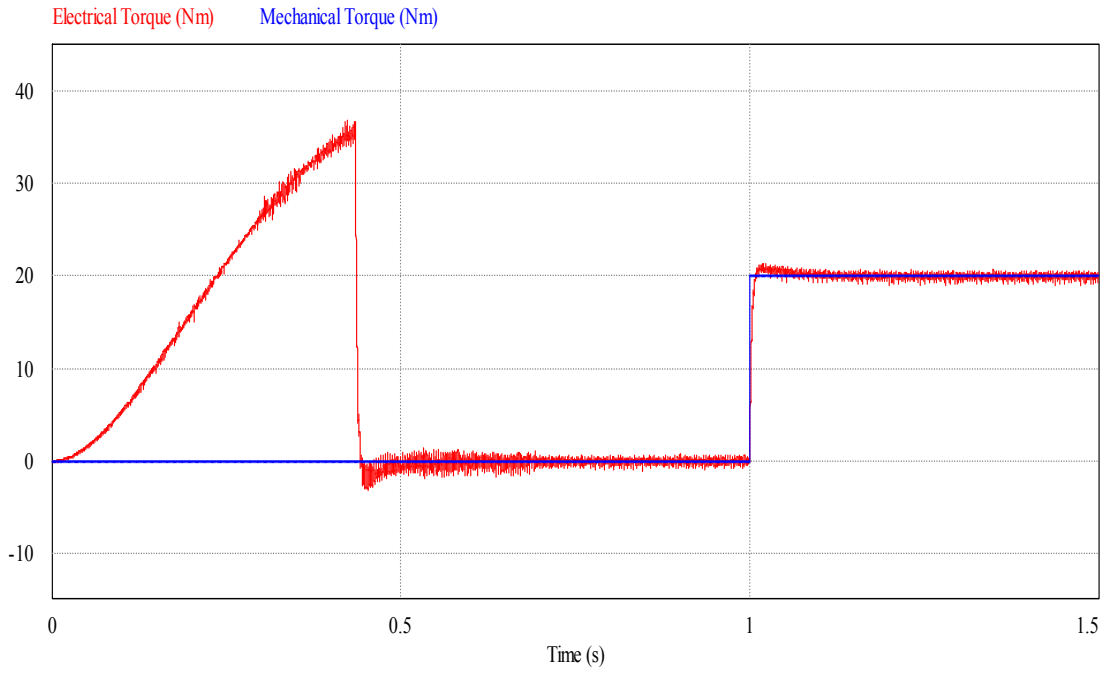

Figure 6.10 Torque response (IFOC)

From the simulation result shown in figure 6.10 it is observed that electrical torque developed during the transit period is limited to the rated value 36Nm. When the machine achieves the steady state the electric torque is equal to the mechanical torque, as is demonstrated in the general equation (5-3) of the machine. The torque contains ripple due to the switching frequency. The ripple value is 2.5%.

The figure 6.10 shows the behavior of the stator currents during the transient and steady state periods. From figure 6.11 can be noted that during the transient period the current is increased until 1.5p.u. During the non load conditions of the machine, the current is remained in 15.8A. When the load is connected at 1 s. the current achieves a value of 20A given by the new electrical torque. The fundamental frequency of the currents is shown in figure 6.12.

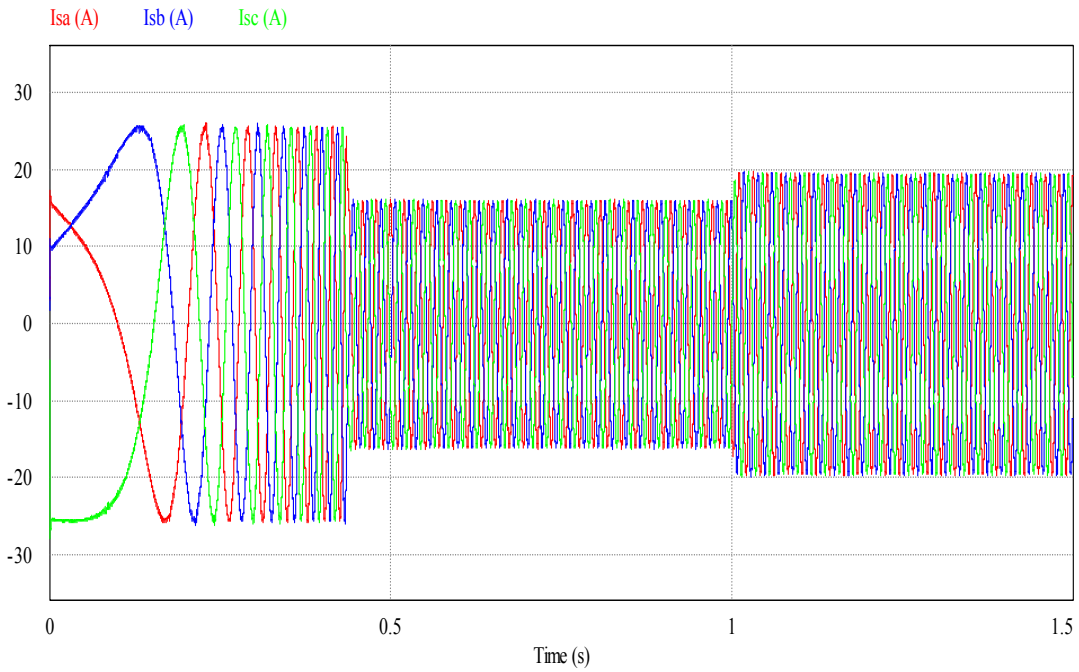

Figure 6.11 Stator currents (IFOC)

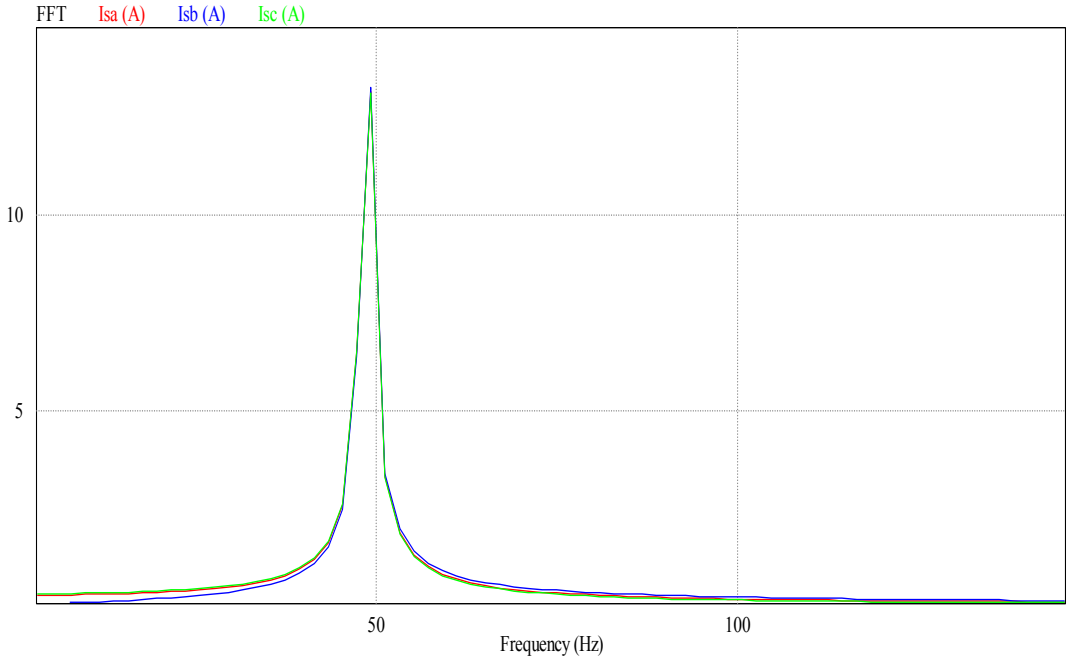

Figure 6.12 Stator currents fundamental frequency (IFOC)

The phase voltage (five levels) generated by the inverter in phase A is presented in figure 6.13. During the transient period only two levels are generated, as soon as the steady state is achieved, the completed levels are formed. The inverter phase voltage contains third harmonics as is shown in figure 6.15 and the THD in steady state is 9%. However using level shifted modulation a reduced in the THD is obtained as is illustrated in chapter 4.

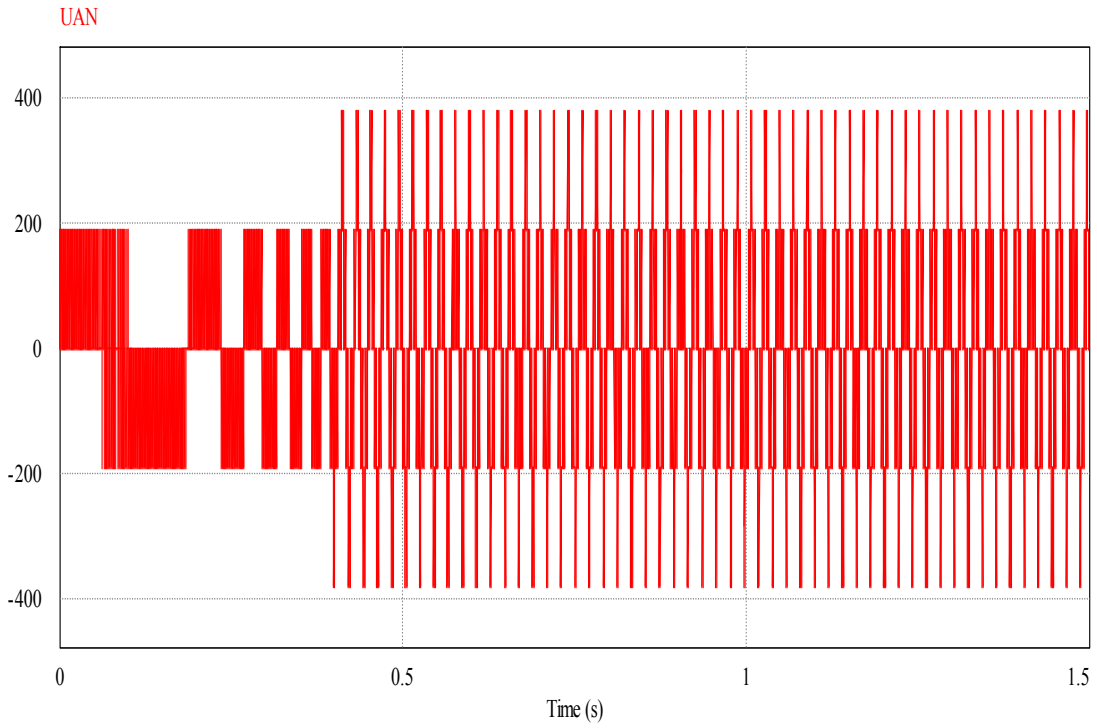

Figure 6.13 Phase voltage waveform (IFOC)

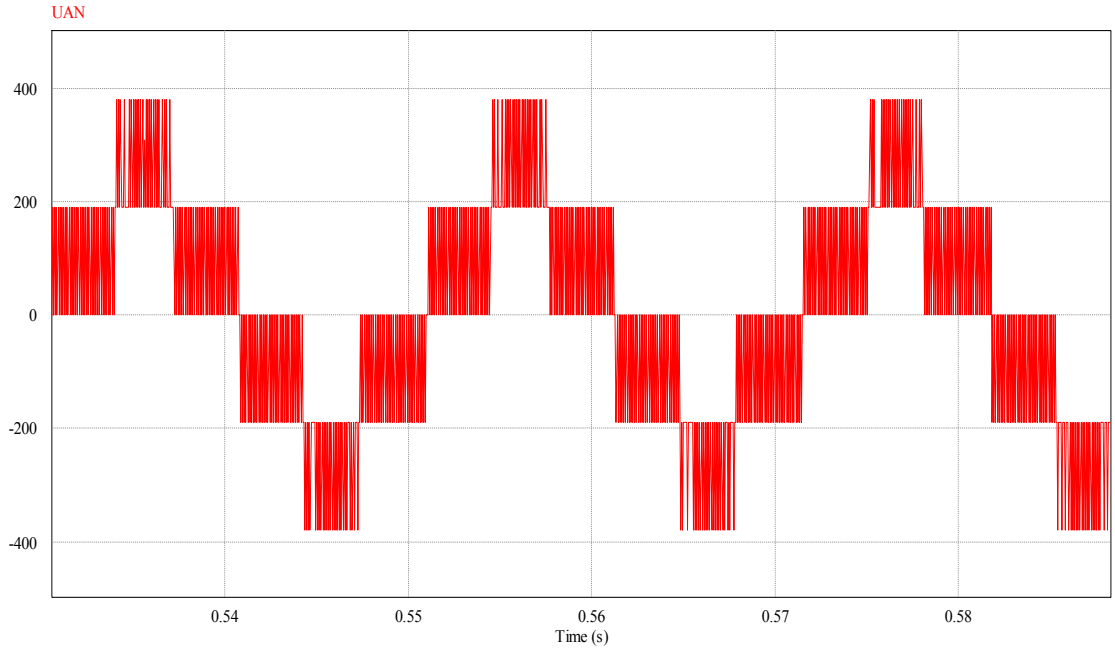

Figure 6.14 Phase voltage waveform in steady state (IFOC)

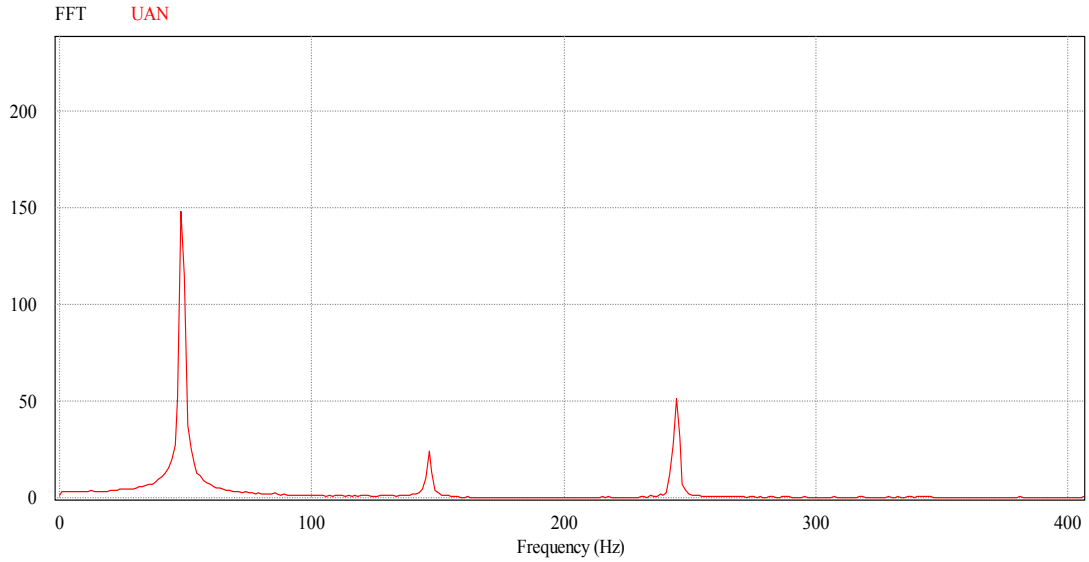

Figure 6.15 Phase voltage harmonic spectrum (IFOC)

6.3 Modified Direct Torque Control (MDTC)

There are many ways to implement a control method based on DTC [5]. However a modified direct torque control is used in the work because of the interest in compare both methods under the same PWM modulation method. The basic scheme of this method described in chapter 5 is presented in figure 6.16.

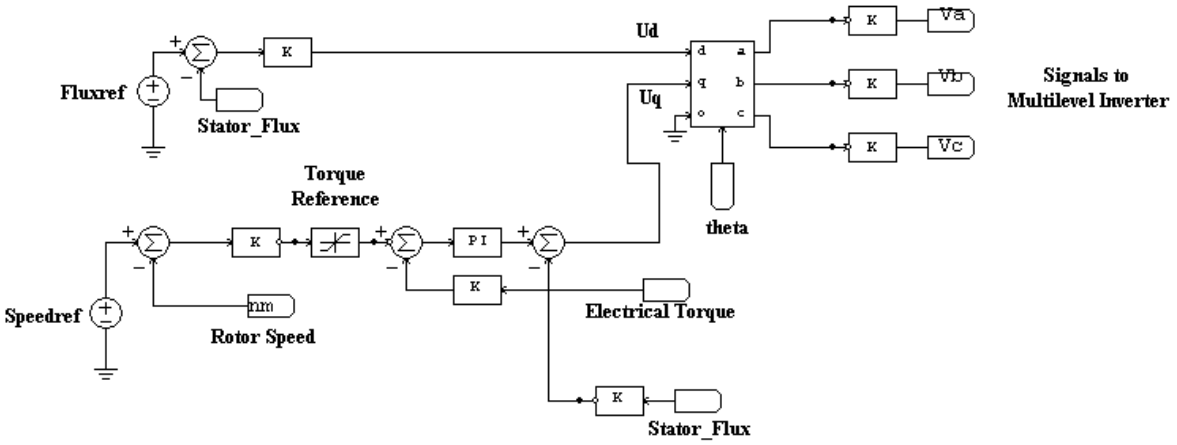

Figure 6.16 Modified direct torque controller implemented in PSIM

In the control shown above, the stator currents and the stator voltages are measured and transformed to a stator frame by using the Clarke transformation, those voltages and currents are used to calculate the stator flux and the electrical torque as follow:

The stator flux vector $\overline{\varphi_s}$ in the stationary frame can be expressed as:

$$\left.\begin{aligned} \overline{\varphi_s} &= \varphi_{\alpha s} + j\varphi_{\beta s} \\ \varphi_{\alpha s} &= \int (U_{\alpha s} - R_s i_{\alpha s})dt \\ \varphi_{\beta s} &= \int (U_{\beta s} - R_s i_{\beta s})dt \end{aligned}\right\} \quad (6\text{-}7)$$

From which it is magnitude and angles are given by:

$$\varphi_s = \sqrt{\varphi_{\alpha s}^2 + \varphi_{\beta s}^2} \quad (6\text{-}8)$$

$$\theta_s = \tan^{-1}\frac{\varphi_{\beta s}}{\varphi_{\alpha s}} \quad (6\text{-}9)$$

Where $U_{\alpha s}$, $U_{\beta s}$, $i_{\alpha s}, i_{\beta s}$ are the measured stator voltages and currents. The developed electric torque can be calculated by:

$$T_e = \frac{3P}{2}(i_{\beta s}\varphi_{\beta s} - i_{\alpha s}\varphi_{\alpha s}) \quad (6\text{-}10)$$

The above equations show that the stator flux and the electric torque can be estimated by using measured stator voltages and currents. The only motor parameter needed in the calculations is the stator resistanceR_s. Unlike the indirect field oriented control, where almost all the parameters are used. The same machine parameters and references described in the indirect field oriented control are used in the modified direct control method.

6.3.1 PI Controllers tuning

The selection of parameters of the PI controllers has been carried out under the same considerations as in the indirect field oriented control. The design of the flux controller is based on equation (5-19) and because of the relation shown in equation (5-25), it is enough with a proportional gain to control the flux during the operation of the machine. This controller set up the reference voltage U_d. The proportional uses the value $K_{p\varphi} = 700$.

The function of the PI controller used in the speed loop is to set the torque reference T_E^*. However the linear relation between the speed and the torque allows using a simple proportional gain to stabilize the speed error and gives fast speed response. The gain setting of this loop controller is K_{pT}= 1.75.

The PI controller used to set the voltage U_q is based on equation (5-20), a paper [6] suggest that the calculation precision of the second term of this equation is not so important, since a PI regulator is present on the torque and it corrects the real value of torque. The gain values of those parameters are $K_p = 0.005$ and $K_i = 0.5$. The generated voltages U_d.and U_q are then transformed to and *abc* reference frame in order to be the input references of the modulation technique.

6.3.2 Simulation Results

As is illustrated in figure 6.16 the machine achieves the rated speed at 0,4 s and it tries to reach the steady state faster than the IFOC method. A constant load of 20 Nm is connected to the machine at 0,5s and the speed drops to 1443 RPM. The control method takes 0,2 s to recover the rated speed as is present in figure 6.18.

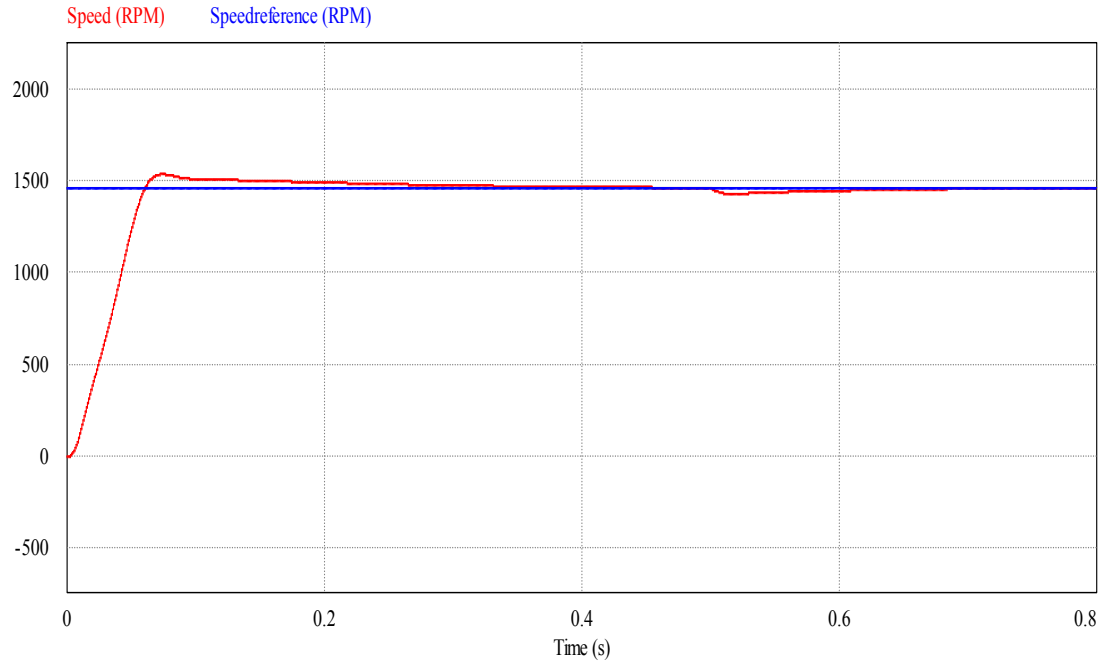

Figure 6.17 Speed response (rated speed=1460RPM) (MDTC)

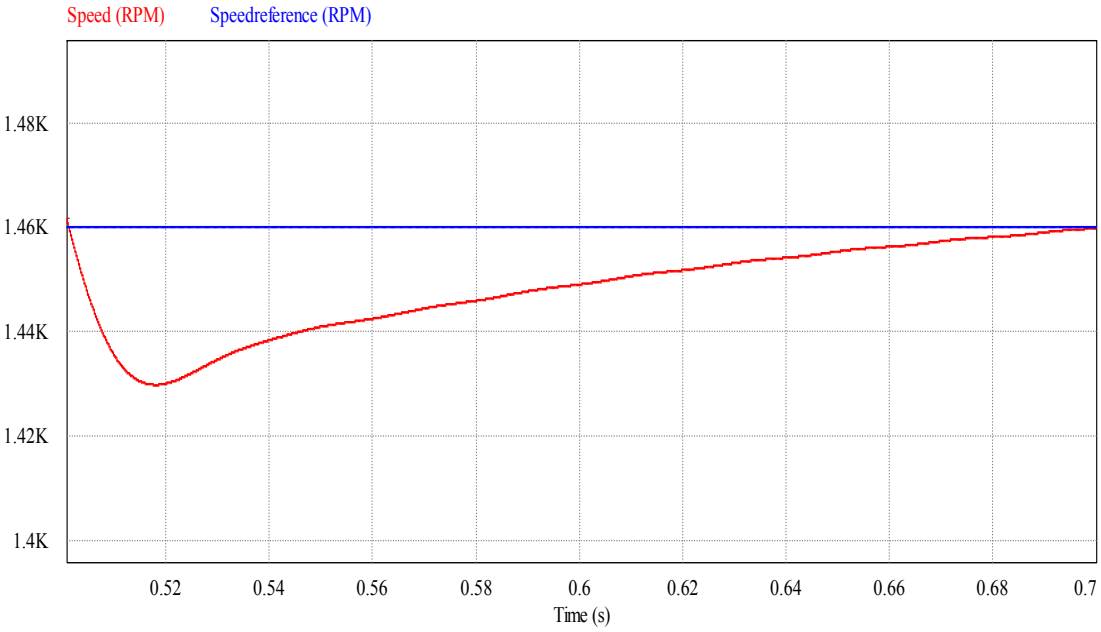

Figure 6.18 Speed variation at t=0,5 s when a load of 20Nm is connected (MDTC)

The figure 6.19 shows the performance of the torque response, a ripple of 10% is presented during the estimation of the electrical torque. During the transient period the torque is limited by the rated torque of the machine.

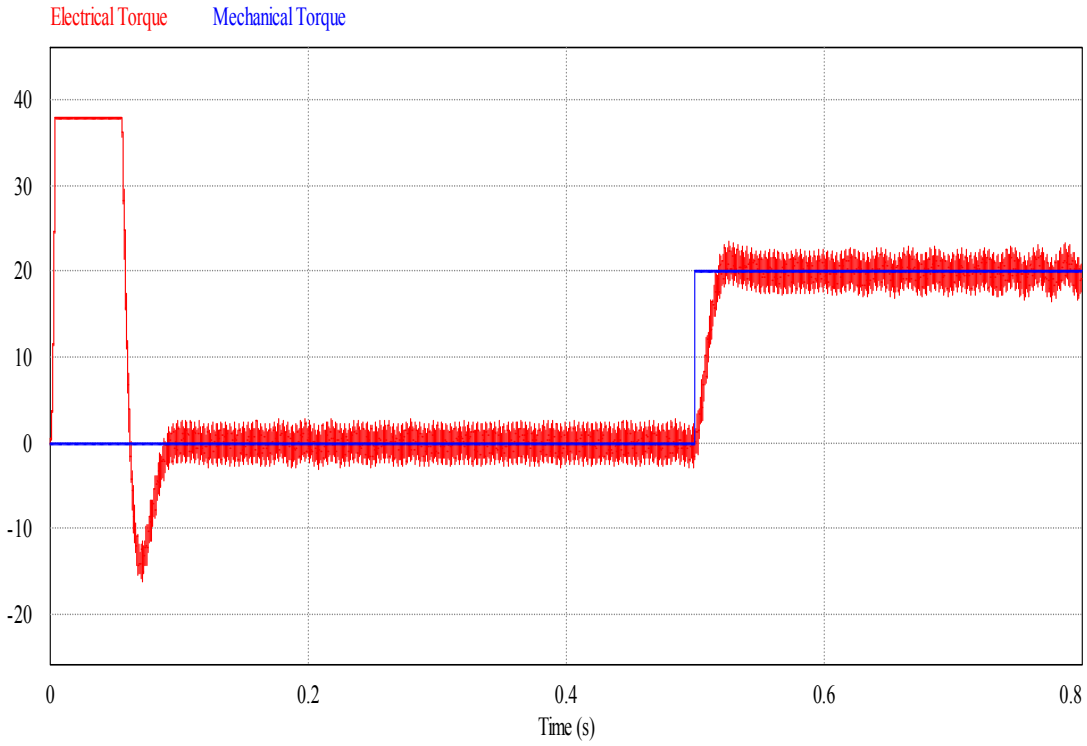

Figure 6.19 Torque response (MDTC)

The torque ripple is one of the drawbacks of the DTC classic method, different proposals such as the increasing the inverter switching frequency have been published in the literature [7][8]. However, due to the processor's inability to operate above certain frequency, there are limitations to increase the switching frequency beyond certain level, without using extra hardware. Therefore, improvements on the modulation technique and controllers have been other alternatives to solve this problem [9].

Figure 6.20 presents the stator currents during the transient and steady state periods. During the transient periods the current is very high and a hysteresis band should be used in order to limit the currents in 1,5 p.u. With help of a Fourier transformation the fundamental frequency is shown in illustrated in figure 6.21.

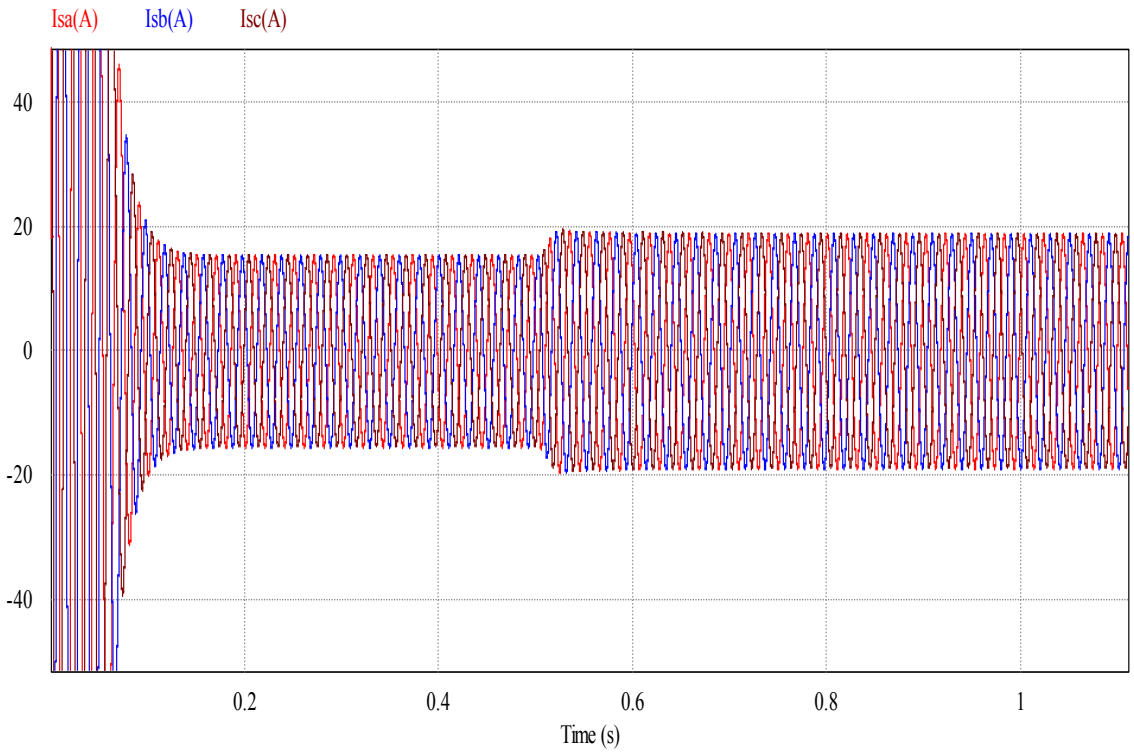

Figure 6.20 Stator currents (MDTC)

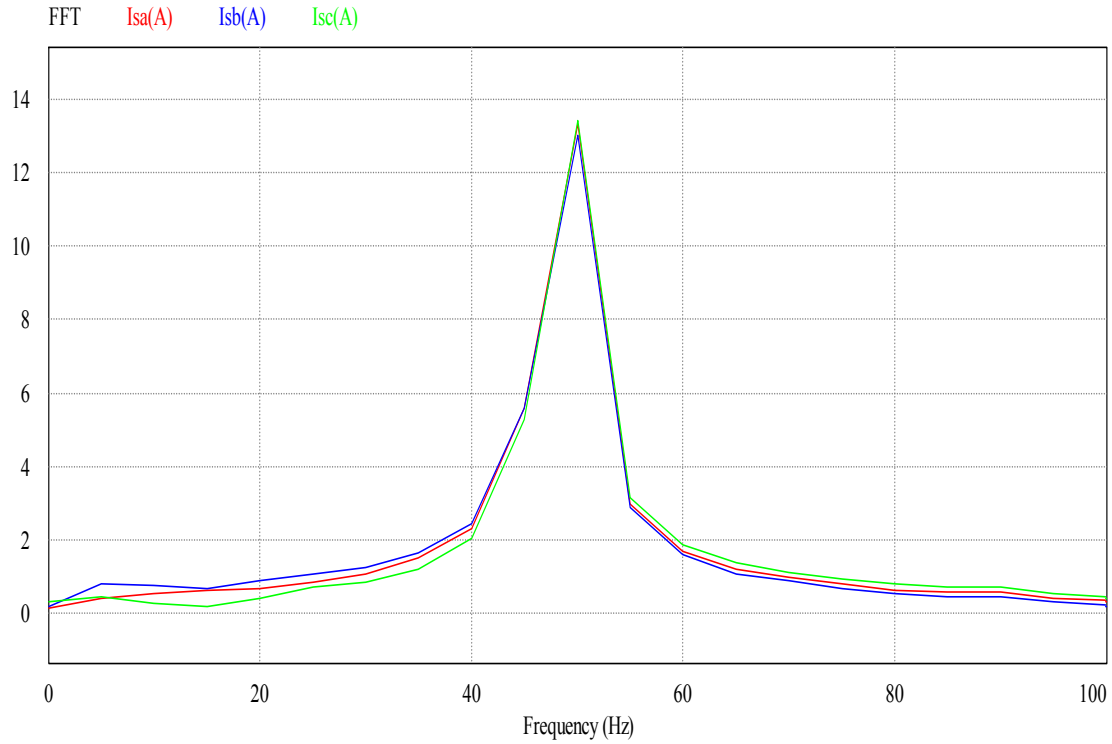

Figure 6.21 Stator currents fundamental frequency (MDTC)

Figures 6.22 and 6.23 present the phase voltage during the transient and steady state periods respectively. As same as the IFOC the complete five voltage levels are formed when the machine reaches the steady state. The THD of the phase voltage is equal to 8,4%.

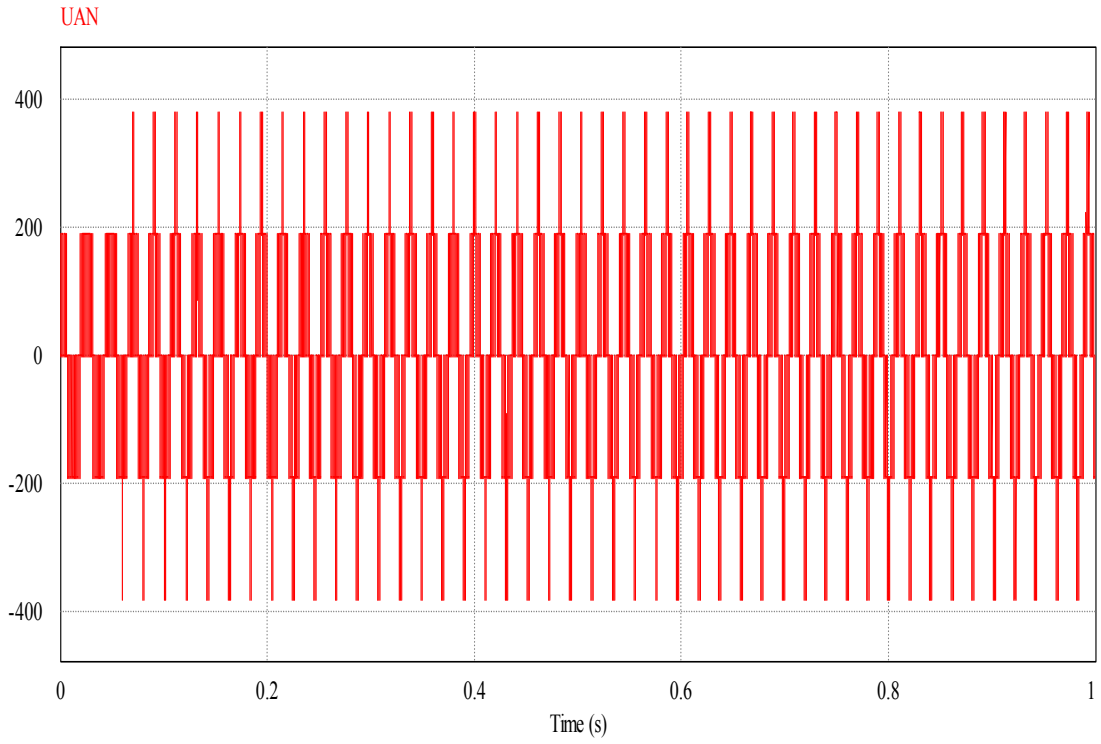

Figure 6.22 Phase voltage waveform (MDTC)

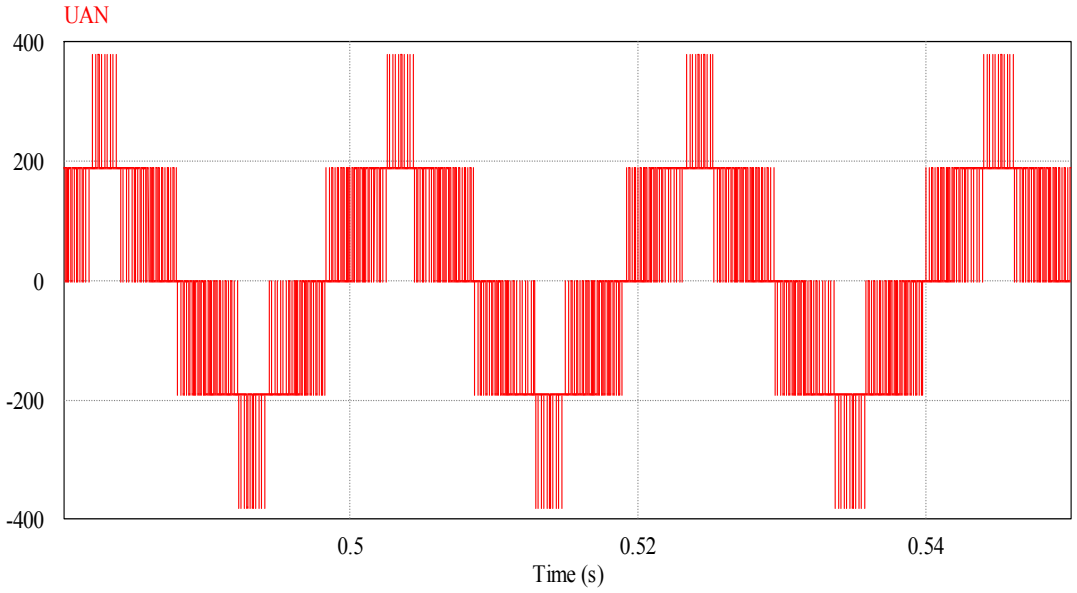

Figure 6.23 Phase voltage waveform in steady state (MDTC)

6.4 Comparison between IFOC and MDTC Methods

With base on the simulation results obtained from the previous sections a comparison between the two schemes is presented in table 6.1.

Comparison	IFOC	MDTC
Motor parameters requiered	*Rs, Lls, Llr, Lm, Rr*	*Rs*
Sensitivity to motor parameter variations	Very sensitive	Not sensitive
Speed controller response	0,16 s	0,2 s
Phase Voltage THD	9 %	8,40 %
Torque ripple	2,50 %	10 %

Table 6.1 Comparison between IFOC and MDTC methods

6.5 References

[1]. Kwon, B.H., Kim, T.W., and Youm, J.H.: 'Novel SVM-based hysteresis current controller', IEEE Trans. Power. Electronics, 1998, 13, (2), pp. 297–307.

[2]. F. Briz, M. Degner, R. Lorentz "Dynamic Analysis of Current Regulators for AC Motors Using Complex Vectors", IEEE Transactions on Industry Applications, vol 35, no 6. November 1999, pp 1424-1432.

[3]. L. Harnefors H-P- Nee "Model-Based Current Control of AC Machines Using the Internal Control Model Method" IEEE Transactions on Industry Applications, Vol 34, No 1, January/ February 1998, pp 133-141.

[4]. J. G. Kassakian, M. F. Schlecht, and G. C. Verghese, "Principles of Power Electronics". Reading, MA: Addison-Wesley, 1991.

[5]. G. S. Buja, M. P. Kazmierkowski "Direct Torque control of PWM inverters AC motors-A survey", IEEE Transcations on Industrial Electronics , vol. 51, no. 4, pp. 744-757. August 2004.

[6]. C. Lascu, I. Boldea, F. Blaabjerg "A modified Direct torque control for Induction Motor Sensorlees Drive" IEEE Transactions on Industry Applications vol, 36 no 1, January-February 2000, pp 122-130.

[7]. C.L.Toh, N. R. N. Idris, and A.H.M.Yatim, "Constant and High Switching Frequency Torque Controller for DTC Drives," IEEE Power Electronics, vol. 03 pp. 76-80, 2005.

[8]. I. Nik Rumzi Nik, Chuen Ling, Toh,Malik, E. Elbuluk, "A New Torque and Flux Controller for Direct Torque Control of Induction Machines " IEEE Transactions and Industrial Applications pp. 1358-1366, 2006.

[9]. S. Pandya, J.K. Chatterjee "Torque Ripple Minimization in Direct Torque Control Based IM Drive Part-I: Single-rate Control Strategy" IEEE 2008.

7. Discussion and Conclusion

A simulation model of systems consisting of a multilevel inverter and an induction machine with a subsea load has been developed. In most applications the motor is fed via a long cable in the range of several tenths of kilometers between the inverter and the motor. However, this system represents the new trend to control the torque and the speed for subsea applications, where the drive and the load are close each other avoiding the drawbacks of having a long cable between them.

The system has been analyzed with the objective to compare two control methods and verify their performance. Results are related to the base case with a cascaded H-bridge five level inverter and 3kW squirrel cage motor. Based on the analysis of such systems the following general conclusions are drawn.

For subsea systems fed by a drive through a long cable, the effects described in chapter 2 such as resonance frequencies, high *dv/dt* on the motor terminal voltages and bearing currents are remedied through the use of appropriate filters. The new trend of having subsea drives appears as a solution for those issues and contributes to improve reliability of PWM motor drive systems.

The main difference between the two control methods can be noted in the sensitivity of the parameters and the torque ripple. The implementation of them demands accurate information on motor parameters. However, parameters such as rotor and stator resistances may vary during operating conditions due to the temperature. In that sense, Modified direct torque control may have a better performance for practical implementations. However for applications where the estimation of the torque is very important, indirect field oriented control may have better results.

Most of the drawbacks mentioned in previous chapters specially those related to torque ripple can be solved using different control techniques and other type of modulation techniques such as space vector modulation. Nowadays there are different ways to implement the two control methods: field oriented control and direct torque control. In modern drives, different alternatives to replace the conventional PI controllers and conventional PWM modulation technique have been replaced by model predictive control and space vector modulation showing with a high performance.

The innovation of more reliable and efficient subsea systems for oil and gas sector is one of the major challenges of the suppliers. The use of appropriate topologies and control systems in power electronics is the key to create new devices demanded by the industry. The induction motor is today the most widely used load for adjustable speed drive applications. This is due to its ruggedness, maintenance and many other advantages compared to other machines. Field Oriented Control and Direct Torque Control have become the standard control solutions to achieve high dynamic performance of the machine. There are many ways to implement both methods. A comparison between two schemes based on conventional PWM has carried out in this thesis. Both control methods require the employment of current loops, PI regulators, coordinates transformations and so on. Based on numerical simulations a good performance

of both controllers was obtained and the whole performance of the two control methods is comparable. Although the thesis is based on a theoretical research, the concepts and applications can be used for other topologies of multilevel inverters and typical medium drives for industrial applications. Moreover, the control methods can be used for Permanent Magnet (PM) synchronous motors which they have been very attractive for certain applications due to the high efficiency, high steady state and torque density.

8. Future Work

Since multilevel inverter fed motor drives have gained special attention in the industry and academia as the preferred choice of electronic power conversion for high power applications, there are still quite a few important aspects to be solved.

First, as the present work has been carried out for a small machine. It can be extended for typical rated values of drives in the industry, up 12MW. It means that an H-bridge cascaded multilevel inverter with four (4) and (6) cells per phase in order to generate the desired voltage of 4,16kV and 6kV respectively are needed. Both control methods have been evaluated with an H-bridge cascaded multilevel inverter. By the use of the other two typical configuration of multilevel inverters: diode-clamped (or neutral-point-clamped) and flying-capacitor the control methods should be developed.

The conventional PWM modulation technique was implemented for both control methods. A comparison with base on space vector modulation technique should be analyzed in order to see the advantages and/or drawbacks in the control performance.

Finally and because of the wide use of DTC and FOC in drives, more efficient inner loop controllers should be explored in order to replace the implemented PI controllers. Model predictive control allows to control a plant within their bounds while optimize a variable of interest. This basic idea can be used to control flux and torque while reduce one of the main concerns in multilevel inverters such as the switching frequency and/or the switching losses and harmonics.

9. Appendixes

The main appendixes are as follows:

Appendix 1

Different types of Control Methods

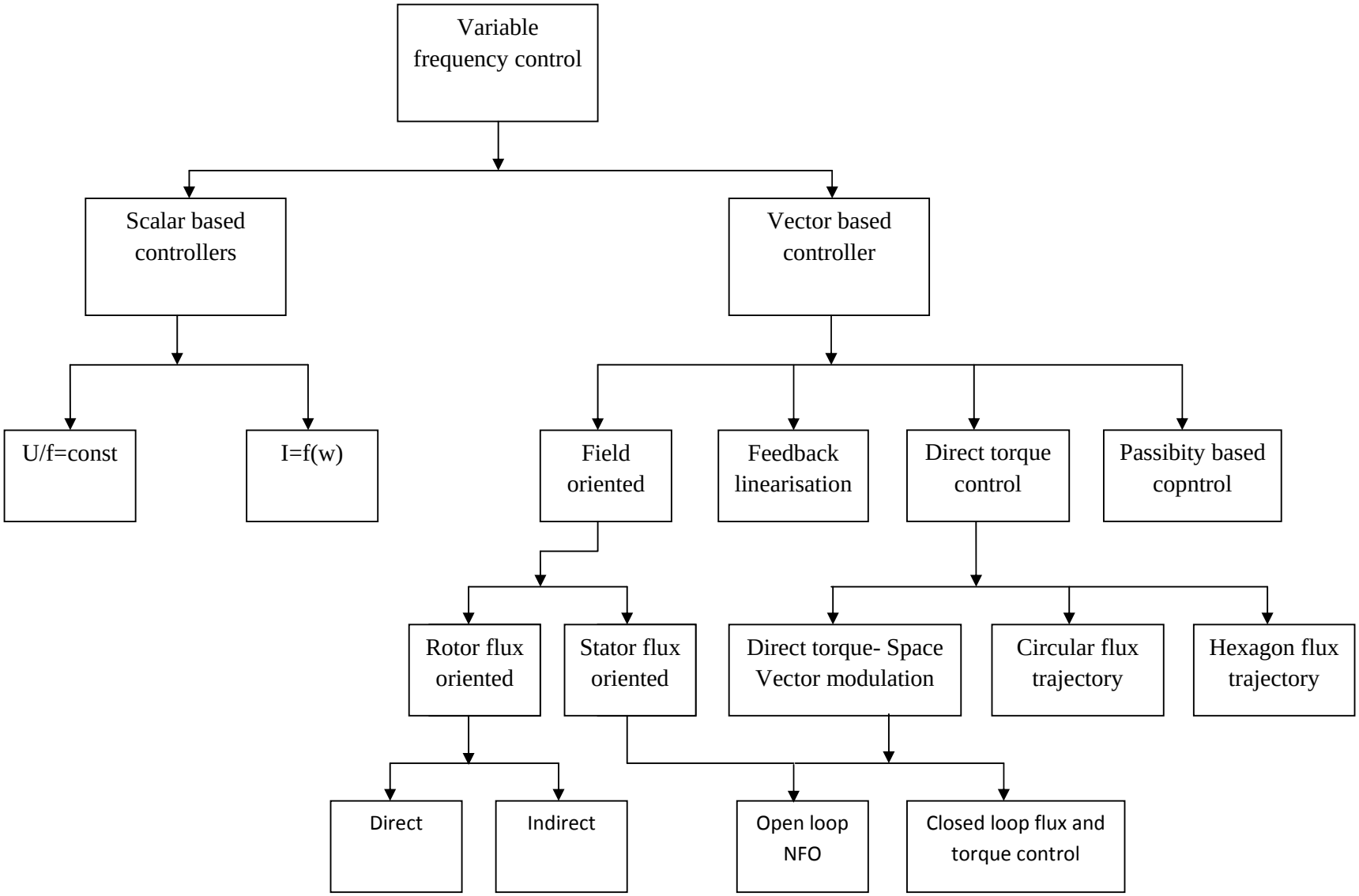

Appendix 2

Phase shifted modulation of a five level H-bridge Cascaded Multilevel Inverter

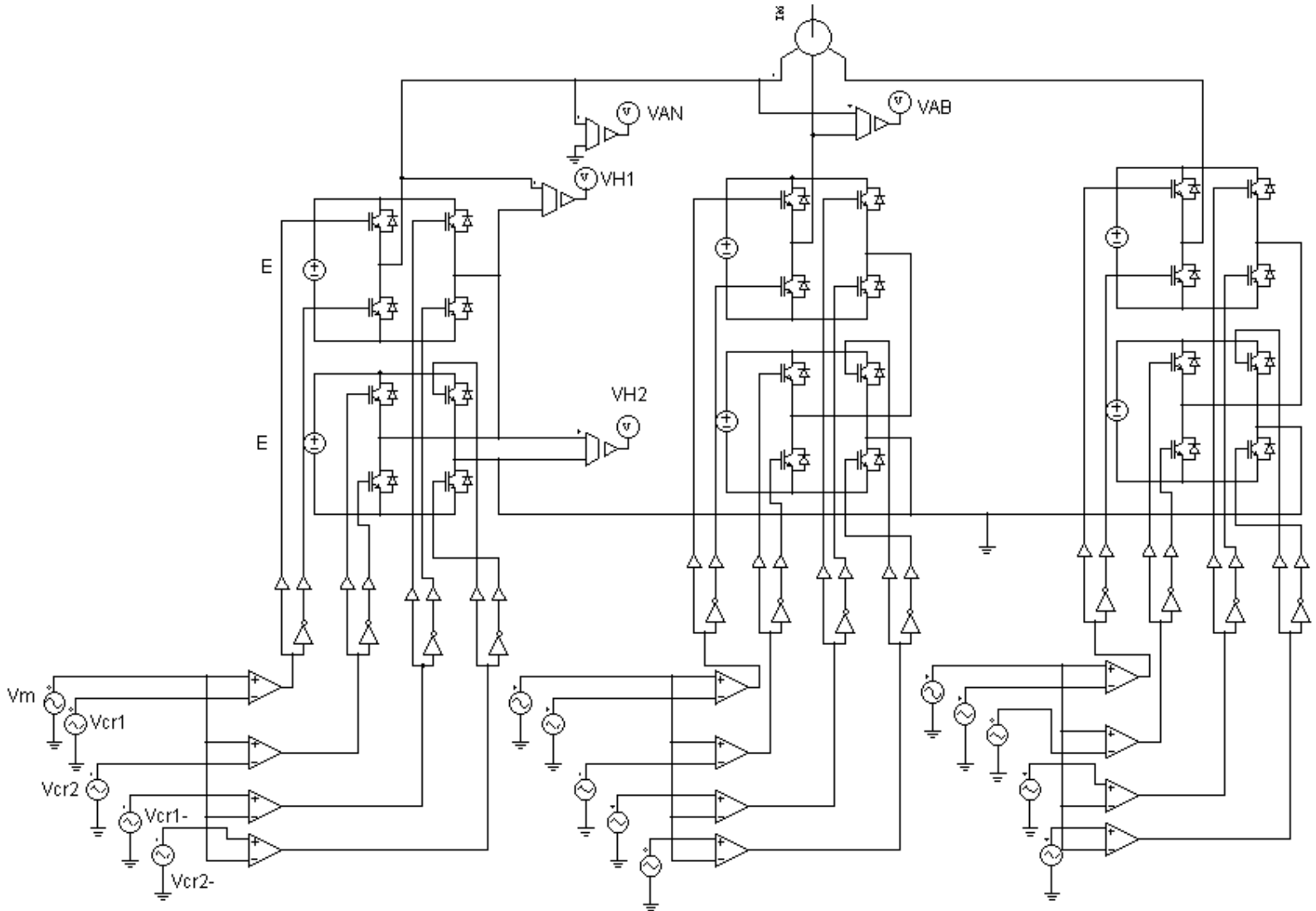

Appendix 3

```
%Tunning PI controller of speed  Indirect Field oriented control

clc
clear all

Rs=0.294;   %Stator resistance
Rr=0.156;   %Rotor resistance
Ls=0.00139; %Stator inductance
Lr=0.00074; %Rotor inductance
Lm=0.041;   %Magnetizing inductance
LR=Lr+Lm;

R=Rs+Rr;
L=Ls+Lr;
Tr=(Lr+Lm)/Rr;% Time constant of Rotor
Id=15.8;

H=Rr/(LR*Id); %Plant transfer function
Kp=1;         %Proportional gain of PI Controller
Ti=0.05;       %Time constant of PI Controller
PI=Kp*(1+tf(1,[Ti 0]));

A=PI*H;
R=A/(1+A);
Iref=1460;
step(R*Iref,1.5)
grid on
```

Appendix 4

```
%Tunning of inner PI Controller for Currents Isd and Isq  (Indirect field oriented control)

clc
clear all


%Motor 460V, 3kW

Rs=0.294;     %Stator resistance
Rr=0.156;     %Rotor resistance
Ls=0.00139;   %Stator inductance
Lr=0.00074;   %Rotor inductance
Lm=0.041;     %Magnetizing inductance
La=Ls-(Lm^2/Lr)

R=Rs+Rr;
L=Ls+Lr;

num=[1];
den=[L R];
H=tf(num,den);

Kp=1;
Ti=0.05;
PI=Kp*(1+tf(1,[Ti 0]))
A=PI*H;
R1=A/(1+A);
Iref=15.8;
step(R1*Iref,0.2)
grid on
```

Appendix 5. Indirect Field Oriented Control Scheme

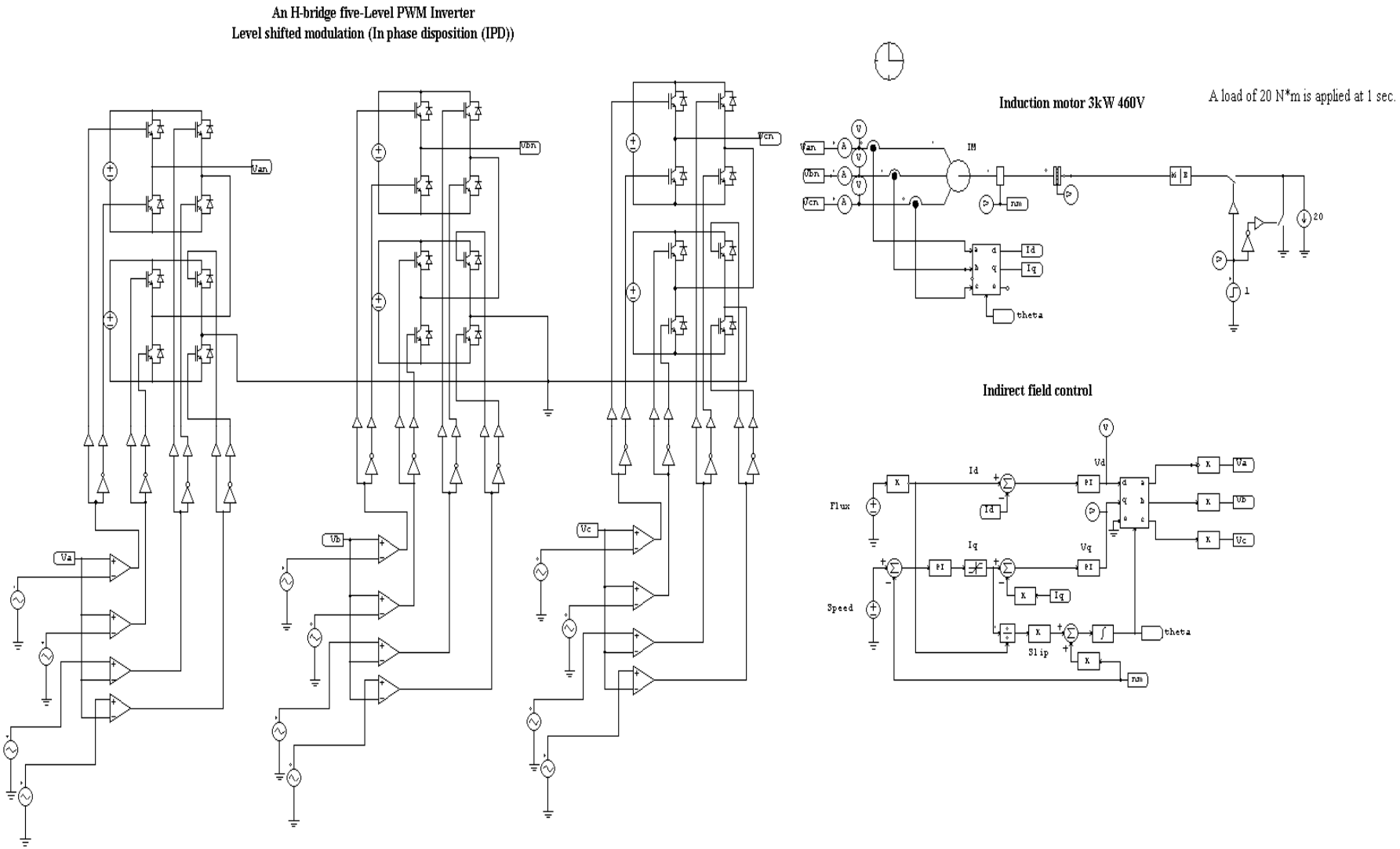

Appendix 6. Modified Direct Torque Control